Published OnlineFirst May 15, 2014; DOI: 10.1158/0008-5472.CAN-14-0241

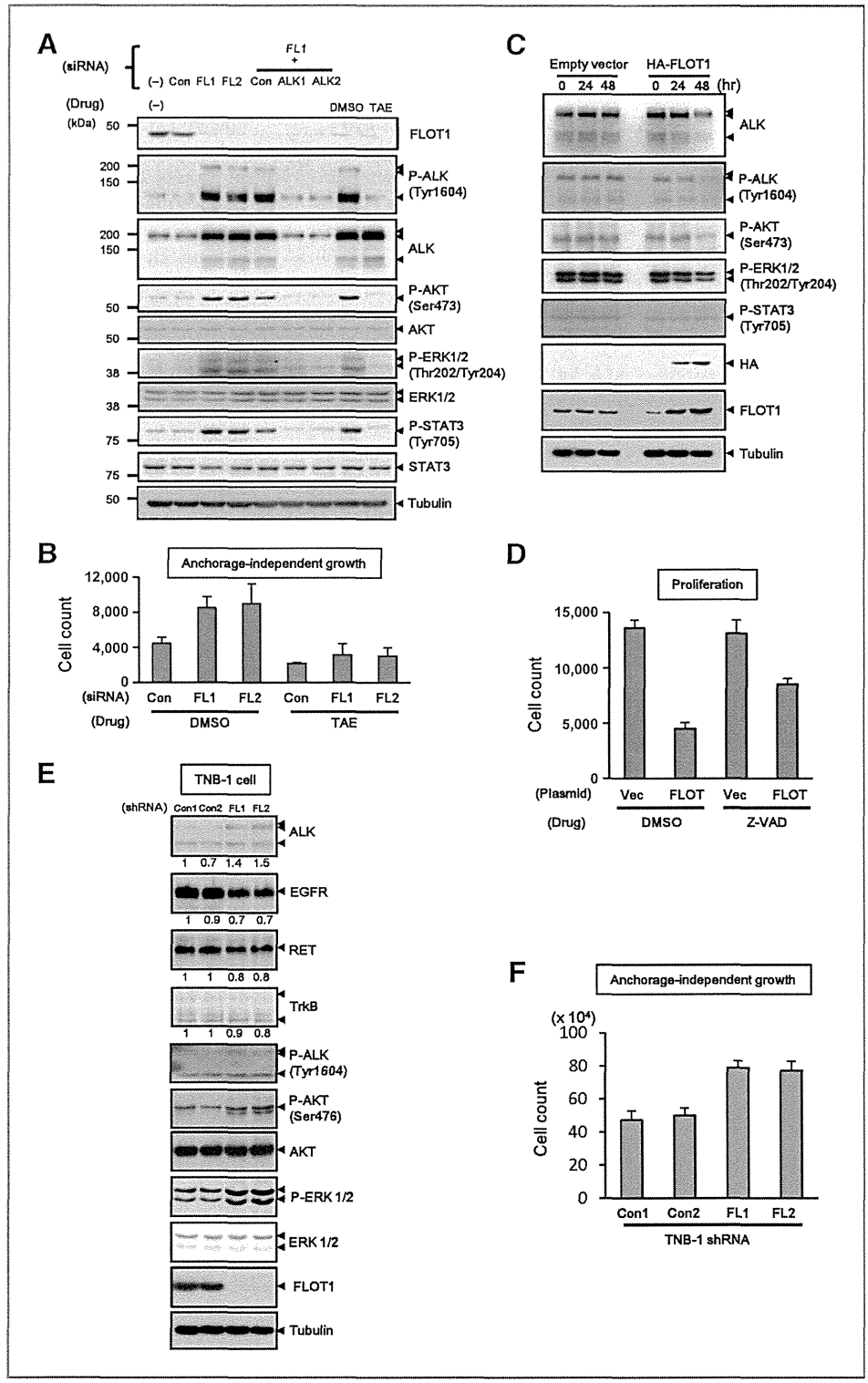

Figure 4. FLOT1 regulates ALK signaling and oncogenicity of neuroblastoma cells. A, NB-39-nu cells were treated with control (Con) or *FLOT1* siRNA (FL1 or FL2) alone or in combination with *ALK* siRNA (ALK1 or ALK2) for 72 hours. *FLOT1* siRNA-treated cells were further cultured in the presence of DMSO or ALK inhibitor NVP-TAE-684 (TAE; 20 nmol/L) for 2 hours. The cell lysates were analyzed by immunoblot analysis using the indicated antibodies. B, NB-39-nu cells were treated with indicated siRNAs and their anchorage-independent growth under continuous treatment with DMSO or TAE was tested as described in Materials and Methods. C, NB-39-nu cells were transiently transfected with an empty vector or HA-tagged FLOT1 for the indicated times. The cell lysates were analyzed by immunoblot analysis using the indicated antibodies. D, NB-39-nu cells transfected with vector alone or HA-tagged FLOT1 were cultured with DMSO or the caspase inhibitor z-VAD-FMK (Z-VAD; 100 μmol/L) for 72 hours. Cell proliferation was measured as described in Materials and Methods. E, stable transfectants of TNB-1 cells expressing control shRNA (TNB-Con1 and TNB-Con2) or FLOT1 shRNA (TNB-FL1 and TNB-FL2) were analyzed by immunoblotting. The expression levels of RTKs were quantified and denoted as relative value (TNB-Con1 = 1) under each immunoblotting data. F, the anchorage-independent growth of TNB-1 cells expressing control or FLOT1 shRNA was tested as described in Materials and Methods.

of endocytosis of ALK, including mode of association between FLOT1 and ALK and the role of tyrosine phosphorylation of FLOT1 in this process. It has been reported that another RTK-binding protein Cbl is involved in the down-regulation of RTKs through receptor ubiquitination followed by endocytosis. Indeed, some mutations in the RTKs, Met and EGFR, decrease the affinity of RTKs with Cbl, which results in impaired endocytosis and oncogenic accumulation of RTKs in several cancers, including lung cancer and glioblastoma (43).

Published OnlineFirst May 15, 2014; DOI: 10.1158/0008-5472.CAN-14-0241

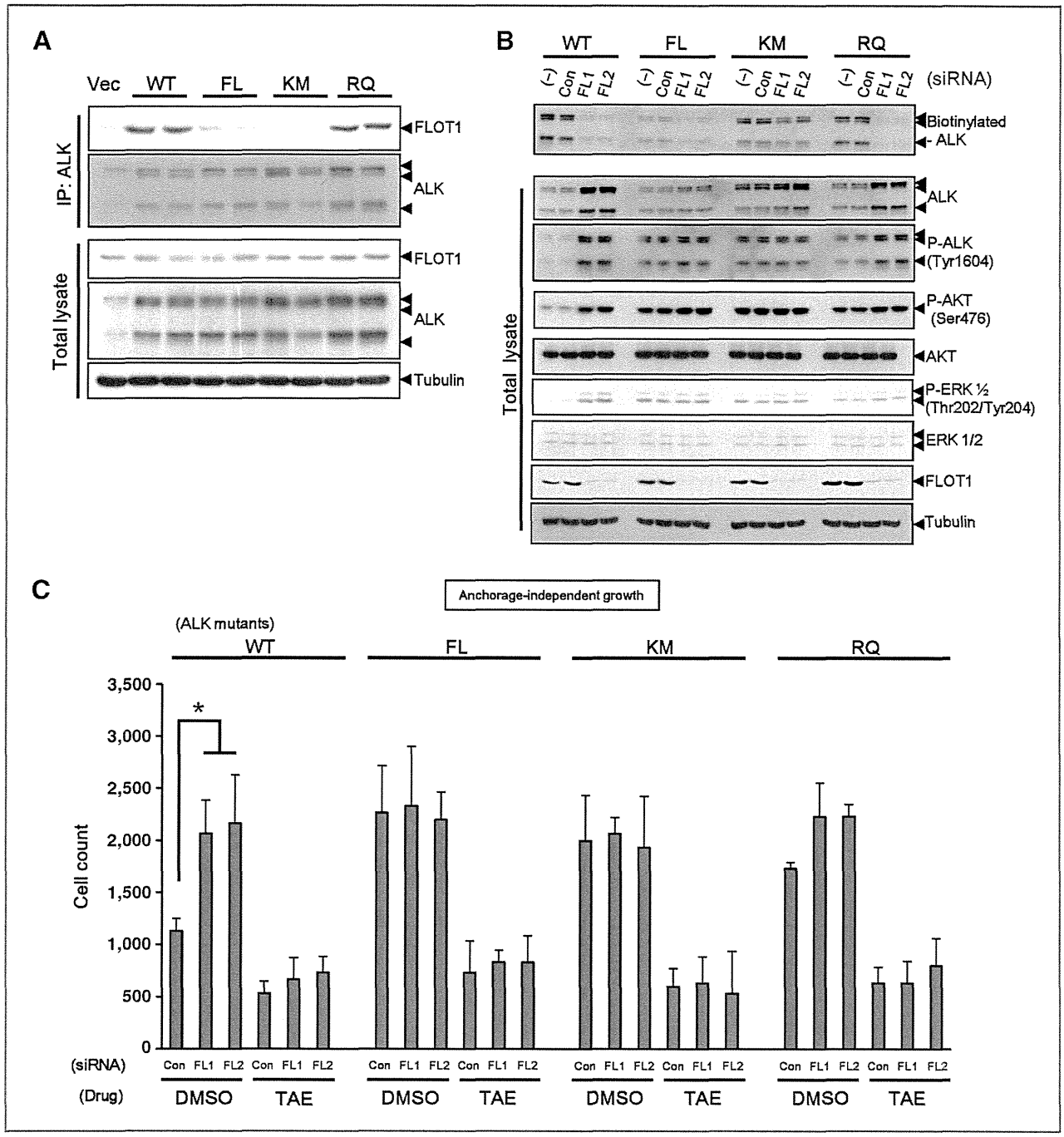

Figure 5. Activating mutations of ALK confer resistance to downregulation by FLOT1. A, cell lysates from each pair of different stable TNB-1 transfectants of empty vector and ALK mutants (WT; FL, F1174L; KM, K1062M; RQ, R1275Q) were immunoprecipitated using the anti-ALK antibody. The immunocomplexes and total cell lysates were analyzed by immunoblotting. B, the stable TNB-1 transfectants were transfected with control siRNA (con) or *FLOT1* siRNA (FL1 or FL2) for 48 hours. The cells were subjected to the ALK internalization assay for 60 minutes, and the internalized proteins and total cell lysates were analyzed by immunoblotting. C, the stable TNB-1 cells transfectants were transfected with indicated siRNAs for 48 hours and cultured in the presence of DMSO or ALK inhibitor NVP-TAE-684 (TAE; 20 nmol/L) for 2 hours. The cells were subjected to the anchorage-independent cell growth assay under continuous treatment with DMSO or TAE. *, $P < 0.01$.

It was recently reported that neuroblastoma cases harboring certain activation mutations of ALK exhibit higher refractoriness (19). For example, neuroblastoma cases harboring the F1174L mutant are also reported to have higher resistance than cases with amplified or R1275Q-mutant ALK when treated with an ALK inhibitor (18). Both the F1174L and R1275Q mutations of

Published OnlineFirst May 15, 2014; DOI: 10.1158/0008-5472.CAN-14-0241

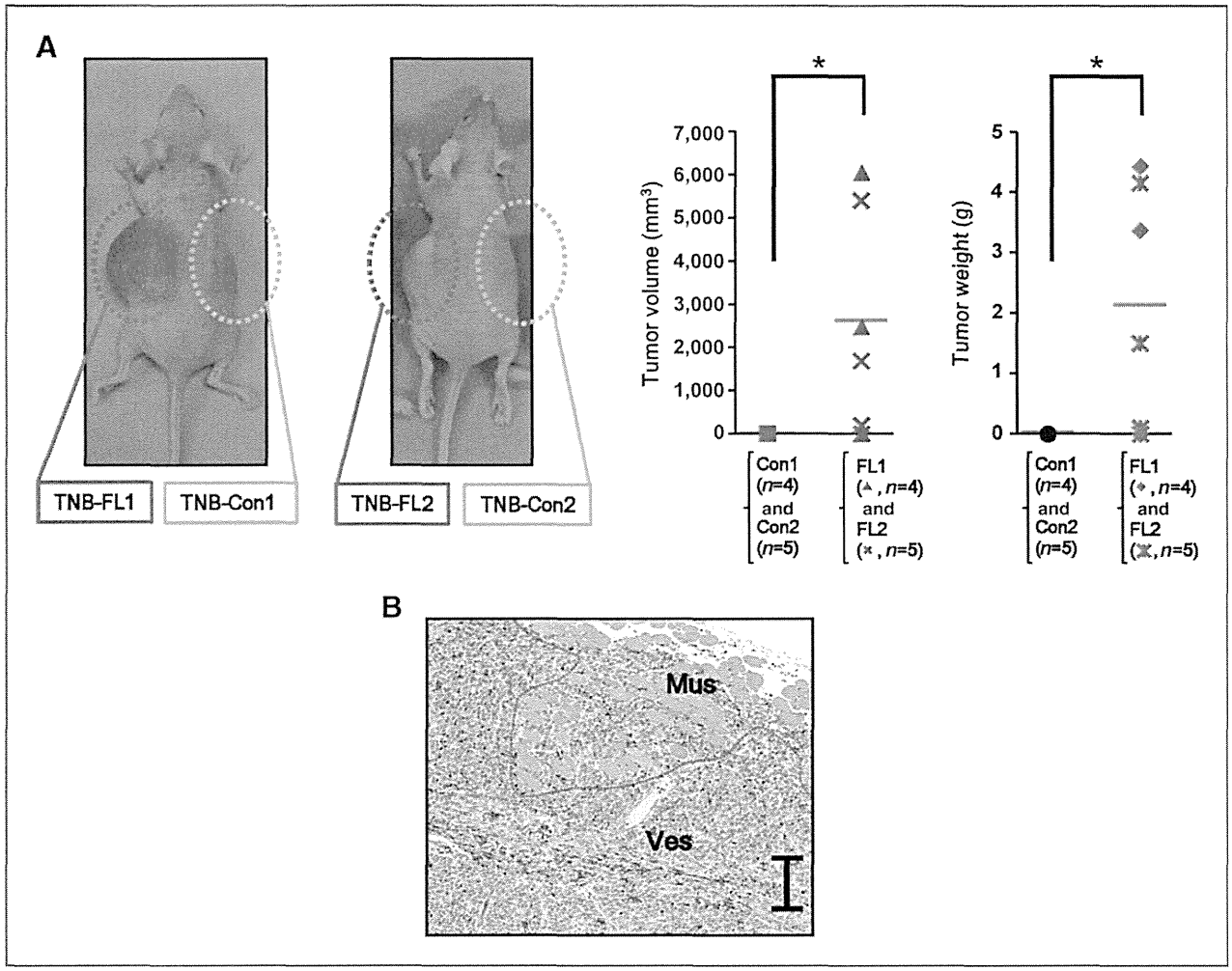

Figure 6. FLOT1 negatively regulates tumorigenicity of neuroblastoma cells. A, left, macroscopic images of the mouse xenograft experiment. The TNB-1 cells stably expressing control (TNB-Con1 and -Con2, yellow circle) or FLOT1 shRNA (TNB-FL1 and -FL2, red circle) were subcutaneously inoculated into both sides of the flank of 4-week-old nude mice as shown (see Supplementary Materials and Methods). In the first group (group 1) TNB-Con1 and -FL1 cells, and in the second group (group 2) TNB-Con2 and -FL2 cells were inoculated. The images of one of the 5 mice from each group 1 and group 2 at 6 weeks after inoculation were presented. Right, the total tumor volume and weight were measured and plotted as scatter grams. Green bars, average values. *, $P < 0.01$. B, high magnification image of the tumor tissue stained with H&E from the mouse (group 1, TNB-FL1 cells). Tumor invasion into the subcutaneous muscle layer (Mus) and the formation of intratumoral large vessels (Ves) were observed. The dotted line denotes the margin of the muscle layer. Bar, 100 μm.

ALK are frequently observed, while F1174L mutant is more aggressive and resistant to ALK inhibitors than R1275Q mutants even in a transgenic fly system (20). We demonstrated that the FL and KM mutants of ALK have less affinity to FLOT1 and therefore less affected by FLOT1-mediated endocytosis than the WT ALK (Fig. 5B). The role of oncogenic potential of ALK mutants has previously been analyzed with respect to ATP-binding potential and impaired receptor trafficking (44, 45), while our results suggest that impaired downregulation of ALK by FLOT1 might contribute to the aggressiveness of some mutations of ALK (Supplementary Fig. S8). It should be emphasized that expression levels of FLOT1 might also become one of the efficient clinical markers determining prognosis and therapeutic effectiveness of ALK inhibitors in neuroblastoma cases.

Disclosure of Potential Conflicts of Interest

No potential conflicts of interests were disclosed.

Authors' Contributions

Conception and design: A. Tomiyama, T. Uekita, R. Kamata, J. Takita, R. Sakai
Development of methodology: A. Tomiyama, J. Takita
Acquisition of data (provided animals, acquired and managed patients, provided facilities, etc.): A. Tomiyama, K. Sasaki, J. Takita, A. Nakagawara
Analysis and interpretation of data (e.g., statistical analysis, biostatistics, computational analysis): A. Tomiyama, T. Uekita, R. Kamata, K. Sasaki, J. Takita, R. Sakai
Writing, review, and/or revision of the manuscript: A. Tomiyama, T. Uekita, J. Takita, H. Yamaguchi, R. Sakai
Administrative, technical, or material support (i.e., reporting or organizing data, constructing databases): A. Tomiyama, T. Uekita, R. Kamata, J. Takita, M. Ohira, A. Nakagawara, C. Kitanaka, R. Sakai
Study supervision: T. Uekita, J. Takita, K. Mori, H. Yamaguchi, R. Sakai

Published OnlineFirst May 15, 2014; DOI: 10.1158/0008-5472.CAN-14-0241

Grant Support

This work was supported by the National Cancer Center Research and Development Fund (25-B-3) and by Grants-in-Aid for Scientific Research (B) by the Ministry of Education, Culture, Sports, and Science and Technology of Japan.

The costs of publication of this article were defrayed in part by the payment of page charges. This article must therefore be hereby marked *advertisement* in accordance with 18 U.S.C. Section 1734 solely to indicate this fact.

Received January 27, 2014; revised May 2, 2014; accepted May 3, 2014; published OnlineFirst May 15, 2014.

References

1. Iwahara T, Fujimoto J, Wen D, Cupples R, Bucay N, Arakawa T, et al. Molecular characterization of ALK, a receptor tyrosine kinase expressed specifically in the nervous system. Oncogene 1997;14:439–49.
2. Morris SW, Kirstein MN, Valentine MB, Dittmer KG, Shapiro DN, Saltman DL, et al. Fusion of a kinase gene, ALK, to a nucleolar protein gene, NPM, in non-hodgkin's lymphoma. Science 1994;263:1281–4.
3. Griffin CA, Hawkins AL, Dvorak C, Henkle C, Ellingham T, Perlman EJ. Recurrent involvement of 2p23 in inflammatory myofibroblastic tumors. Cancer Res 1999;59:2776–80.
4. Jazii FR, Najafi Z, Malekzadeh R, Conrads TP, Ziaee AA, Abnet C, et al. Identification of squamous cell carcinoma associated proteins by proteomics and loss of beta tropomyosin expression in esophageal cancer. World J Gastroenterol 2006;12:7104–12.
5. Lin E, Li L, Guan Y, Soriano R, Rivers CS, Mohan S, et al. Exon array profiling detects EML4-ALK fusion in breast, colorectal, and non-small cell lung cancers. Mol Cancer Res 2009;7:1466–76.
6. Soda M, Choi YL, Enomoto M, Takada S, Yamashita Y, Ishikawa S, et al. Identification of the transforming EML4-ALK fusion gene in non-small-cell lung cancer. Nature 2007;448:561–6.
7. Cazes A, Louis-Brennetot C, Mazot P, Dingli F, Lombard B, Boeva V, et al. Characterization of rearrangements involving the ALK gene reveals a novel truncated form associated with tumor aggressiveness in neuroblastoma. Cancer Res 2013;73:195–204.
8. Chen Y, Takita J, Choi YL, Kato M, Ohira M, Sanada M, et al. Oncogenic mutations of ALK kinase in neuroblastoma. Nature 2008;455:971–4.
9. George RE, Sanda T, Hanna M, Frohling S, Luther W II, Zhang J, et al. Activating mutations in ALK provide a therapeutic target in neuroblastoma. Nature 2008;455:975–8.
10. Janoueix-Lerosey I, Lequin D, Brugieres L, Ribeiro A, de Pontual L, Combaret V, et al. Somatic and germline activating mutations of the ALK kinase receptor in neuroblastoma. Nature 2008;455:967–70.
11. Mosse YP, Laudenslager M, Longo L, Cole KA, Wood A, Attiyeh EF, et al. Identification of ALK as a major familial neuroblastoma predisposition gene. Nature 2008;455:930–5.
12. Okubo J, Takita J, Chen Y, Oki K, Nishimura R, Kato M, et al. Aberrant activation of ALK kinase by a novel truncated form ALK protein in neuroblastoma. Oncogene 2012;31:4667–76.
13. Osajima-Hakomori Y, Miyake I, Ohira M, Nakagawara A, Nakagawa A, Sakai R. Biological role of anaplastic lymphoma kinase in neuroblastoma. Am J Pathol 2005;167:213–22.
14. De Bernardi B, Nicolas B, Boni L, Indolfi P, Carli M, Cordero Di Montezemolo L, et al. Disseminated neuroblastoma in children older than one year at diagnosis: comparable results with three consecutive high-dose protocols adopted by the italian co-operative group for neuroblastoma. J Clin Oncol 2003;21:1592–601.
15. Matthay KK, Villablanca JG, Seeger RC, Stram DO, Harris RE, Ramsay NK, et al. Treatment of high-risk neuroblastoma with intensive chemotherapy, radiotherapy, autologous bone marrow transplantation, and 13-cis-retinoic acid. Children's cancer group. N Engl J Med 1999;341:1165–73.
16. Pearson AD, Pinkerton CR, Lewis IJ, Imeson J, Ellershaw C, Machin D, et al. High-dose rapid and standard induction chemotherapy for patients aged over 1 year with stage 4 neuroblastoma: a randomised trial. Lancet Oncol 2008;9:247–56.
17. Mosse YP, Lim MS, Voss SD, Wilner K, Ruffner K, Laliberte J, et al. Safety and activity of crizotinib for paediatric patients with refractory solid tumours or anaplastic large-cell lymphoma: a children's oncology group phase 1 consortium study. Lancet Oncol 2013;14:472–80.
18. Bresler SC, Wood AC, Haglund EA, Courtright J, Belcastro LT, Plegaria JS, et al. Differential inhibitor sensitivity of anaplastic lymphoma kinase variants found in neuroblastoma. Sci Transl Med 2011;3:108ra114.
19. De Brouwer S, De Preter K, Kumps C, Zabrocki P, Porcu M, Westerhout EM, et al. Meta-analysis of neuroblastomas reveals a skewed ALK mutation spectrum in tumors with MYCN amplification. Clin Cancer Res 2010;16:4353–62.
20. Schonherr C, Ruuth K, Yamazaki Y, Eriksson T, Christensen J, Palmer RH, et al. Activating ALK mutations found in neuroblastoma are inhibited by crizotinib and NVP-TAE684. Biochem J 2011;440:405–13.
21. Ambrogio C, Voena C, Manazza AD, Piva R, Riera L, Barberis L, et al. p130Cas mediates the transforming properties of the anaplastic lymphoma kinase. Blood 2005;106:3907–16.
22. Miyake I, Hakomori Y, Shinohara A, Gamou T, Saito M, Iwamatsu A, et al. Activation of anaplastic lymphoma kinase is responsible for hyperphosphorylation of ShcC in neuroblastoma cell lines. Oncogene 2002;21:5823–34.
23. Amaddii M, Meister M, Banning A, Tomasovic A, Mooz J, Rajalingam K, et al. Flotillin-1/reggie-2 protein plays dual role in activation of receptor-tyrosine kinase/mitogen-activated protein kinase signaling. J Biol Chem 2012;287:7265–78.
24. Browman DT, Hoegg MB, Robbins SM. The SPFH domain-containing proteins: more than lipid raft markers. Trends Cell Biol 2007;17:394–402.
25. Cremona ML, Matthies HJ, Pau K, Bowton E, Speed N, Lute BJ, et al. Flotillin-1 is essential for PKC-triggered endocytosis and membrane microdomain localization of DAT. Nat Neurosci 2011;14:469–77.
26. Riento K, Frick M, Schafer I, Nichols BJ. Endocytosis of flotillin-1 and flotillin-2 is regulated by FYN kinase. J Cell Sci 2009;122:912–8.
27. Pust S, Klokk TI, Musa N, Jenstad M, Risberg B, Erikstein B, et al. Flotillins as regulators of ErbB2 levels in breast cancer. Oncogene 2013;32:3443–51.
28. Zhang SH, Wang CJ, Shi L, Li XH, Zhou J, Song LB, et al. High Expression of FLOT1 is associated with progression and prognosis in hepatocellular carcinoma. PLos ONE 2013;8:e64709.
29. Xiong P, Xiao LY, Yang R, Guo Q, Zhao YQ, Li W, et al. Flotillin-1 promotes cell growth and metastasis in oral squamous cell carcinoma. Neoplasma 2013;60:395–405.
30. Ikeda I, Ishizaka Y, Tahira T, Suzuki T, Onda M, Sugimura T, et al. Specific expression of the ret proto-oncogene in human neuroblastoma cell lines. Oncogene 1990;5:1291–6.
31. Tuchida Y, Sekiguchi M, Kaneko Y, Kanda N. Origin of human neuroblastoma cell lines TGW and TNB1. FEBS Lett 1990;263:191.
32. Miyake I, Ohira M, Nakagawara A, Sakai R. Distinct role of ShcC docking protein in the differentiation of neuroblastoma. Oncogene 2009;28:662–73.
33. Uekita T, Jia L, Narisawa-Saito M, Yokota J, Kiyono T, Sakai R. Cub domain-containing protein 1 is a novel regulator of anoikis resistance in lung adenocarcinoma. Mol Cell Biol 2007;27:7649–60.
34. Crockett DK, Lin Z, Elenitoba-Johnson KS, Lim MS. Identification of NPM-ALK interacting proteins by tandem mass spectrometry. Oncogene 2004;23:2617–29.
35. Brodeur GM, Nakagara A. Molecular basis of clinical heterogeneity in neuroblastoma. Am J Pediatr Hematol Oncol 1992;14:111–6.
36. Ohira M, Morohashi A, Inuzuka H, Shishikura T, Kawamoto T, Kageyama H, et al. Expression profiling and characterization of

Published OnlineFirst May 15, 2014; DOI: 10.1158/0008-5472.CAN-14-0241

4200 genes cloned from primary neuroblastomas: identification of 305 genes differentially expressed between favorable and unfavorable subsets. Oncogene 2003;22:5525–36.

37. Leithe E, Sirnes S, Fykerud T, Kjenseth A, Rivedal E. Endocytosis and post-endocytic sorting of connexisins. Biochim Biophys Acta 2012;1818:1870–9.
38. Glebov OO, Bright NA, Nichols BJ. Flotillin-1 defines a clathrin-independent endocytic pathway in mammalian cells. Nat Cell Biol 2006; 8:46–54.
39. Rajendran L, Le Lay S, Illges H. Raft association and lipid droplet targeting of flotillins are independent of caveolin. Biol Chem 2007; 388:307–14.
40. Song L, Gong H, Lin C, Wang C, Liu L, Wu J, et al. Flotillin-1 promotes tumor necrosis factor-alpha receptor signaling and activation of NF-kappaB in esophageal squamous cell carcinoma cells. Gastroenterology 2012;143:995–1005 e1012.
41. Kato N, Nakanishi M, Hirashima N. Flotillin-1 regulates IgE receptor-mediated signaling in rat basophilic leukemia (RBL-2H3) cells. J Immunol 2006;177:147–54.
42. Lin C, Wu Z, Lin X, Yu C, Shi T, Zeng Y, et al. Knockdown of FLOT1 impairs cell proliferation and tumorigenicity in breast cancer through upregulation of FOXO3a. Clin Cancer Res 2011;17: 3089–99.
43. Abella JV, Park M. Breakdown of endocytosis in the oncogenic activation of receptor tyrosine kinases. Am J Physiol Endocrinol Metab 2009;296:E973–84.
44. Lee CC, Jia Y, Li N, Sun X, Ng K, Ambing E, et al. Crystal structure of the ALK (anaplastic lymphoma kinase) catalytic domain. Biochem J 2010;430:425–37.
45. Mazot P, Cazes A, Boutterin MC, Figueiredo A, Raynal V, Combaret V, et al. The constitutive activity of the ALK mutated at positions F1174 or R1275 impairs receptor trafficking. Oncogene 2011;30:2017–25.

Published OnlineFirst May 15, 2014; DOI: 10.1158/0008-5472.CAN-14-0241

AACR American Association for Cancer Research

Cancer Research

The Journal of Cancer Research (1916–1930) | The American Journal of Cancer (1931–1940)

Flotillin-1 Regulates Oncogenic Signaling in Neuroblastoma Cells by Regulating ALK Membrane Association

Arata Tomiyama, Takamasa Uekita, Reiko Kamata, et al.

Cancer Res 2014;74:3790-3801. Published OnlineFirst May 15, 2014.

Oncogene (2014) **33,** 2601–2609

www.nature.com/onc

ORIGINAL ARTICLE

RUNX3 interacts with MYCN and facilitates protein degradation in neuroblastoma

F Yu[1,2,3], W Gao[1,4], T Yokochi[1], Y Suenaga[1], K Ando[1], M Ohira[5], Y Nakamura[1] and A Nakagawara[1,2]

RUNX3, a runt-related transcription factor, has a crucial role in dorsal root ganglion neurogenesis. Recent studies have suggested that RUNX3 acts as a tumor suppressor in stomach, colon and breast cancer. However, the biological role of RUNX3 in neuroblastoma remains elusive. Here we report that high levels of *RUNX3* expression contribute to the favorable outcome in patients with neuroblastoma, whereas low levels of *RUNX3* expression result in poor outcome. Array-based analysis suggested that the allelic loss at chromosome 1p36 is one of the reasons why expression of *RUNX3* is downregulated in advanced neuroblastomas. Interestingly, the several patients survived from neuroblastoma with both high mRNA expressions of *MYCN* and *RUNX3*, suggesting that *RUNX3* high expression might overcome the aggressive behavior of *MYCN*. Exogenous expression of *RUNX3* strongly inhibits cell proliferation and migration in neuroblastoma cell lines. Furthermore, RUNX3 reduces the stability of MYCN protein in *MYCN*-amplified neuroblastoma cell lines, and this RUNX3-mediated MYCN degradation may depend on the physical interaction between RUNX3 and MYCN. Thus, our findings provide a tumor-suppressing mechanism by which RUNX3 inhibits the MYCN activity in neuroblastoma.

Oncogene (2014) **33,** 2601–2609; doi:10.1038/onc.2013.221; published online 15 July 2013

Keywords: RUNX3; MYCN; neuroblastoma; tumor suppressor

INTRODUCTION

Human neuroblastoma, a neoplasm of peripheral neural crest origin, is the most common extracranial solid tumor of childhood and accounts for 15% of cancer deaths in children.[1,2] Despite recent advances in treatment options, aggressive neuroblastoma remains refractory to current therapy. The overall 5-year survival rate for patients with advanced-stage of neuroblastoma is 30–40%.[3–5] Neuroblastoma patients harboring genomic *MYCN* amplification accompanied by allelic deletion of short arm of chromosome 1 are at high risk for unfavorable outcome. Amplification of the proto-oncogene *MYCN* occurs in up to 25% of neuroblastoma, strongly correlating to the advanced-stage disease and the failure of chemotherapy treatment.[6–8] Loss of heterozygosity at 1p36 is found in 20–40% of neuroblastoma cases and is independently associated with progression-free survival. Thus, it has been predicted that candidates of tumor-suppressor gene may exist in this region.[9–11]

RUNX3 belongs to the Runt-related gene family, whose members are pivotal regulators of neuronal development.[12,13] *RUNX3* is located at human chromosome 1p36 and its gene product acts as a tumor suppressor in various cancers[14–18] except neuroblastoma. A possible role of RUNX3 in neuroblastoma is suggested by its transcriptional regulation of *TrkB*, which was identified as an oncogene.[19–22] Although the most neuroblastoma cell lines do not synthesize RUNX3 protein at detectable levels, exogenous expression of *RUNX3* causes the cell death, cell cycle arrest or differentiation in neuroblastoma.[23] In this study, we quantitatively measured the expression levels of *RUNX3* in 110 primary neuroblastoma samples to test the hypothesis that the inactivation of *RUNX3* is independently prognostic for adverse stages of the disease. Based on clinical analyses, investigation *in vitro* revealed a reliable mechanism by which RUNX3 inhibits the stability and oncogenic activity of MYCN in neuroblastoma.

RESULTS

Decreased expression of *RUNX3* is associated with poor prognosis in neuroblastoma patients

As the *RUNX3* gene is mapped to chromosome 1p36.2, which is frequently deleted in unfavorable neuroblastomas as well as other cancers, we asked whether *RUNX3* could act as a tumor-suppressor gene in neuroblastoma. We then examined the expression levels of *RUNX3* mRNA in 16 favorable (stage 1 or 2, single copy of *MYCN* and high expression of *TrkA*) and 16 unfavorable (stage 3 or 4, amplification of *MYCN* and low expression of *TrkA*) neuroblastoma samples by semiquantitative reverse transcription–PCR (RT–PCR).[24–27] *RUNX3* was expressed at higher levels in the favorable group than the unfavorable group (Figure 1a). This result prompted us to quantitatively measure the expression levels of *RUNX3* in 110 primary samples of neuroblastomas utilizing real-time PCR. We found that *RUNX3* expression levels in stage 1 and 2 patients tended to be higher (Figure 1b). To further understand the impact of *RUNX3* expression on patients outcome, we divided the clinical samples into two, such as *RUNX3* high ($n = 22$) and low ($n = 88$) expression groups, based on the mean value of *RUNX3* expression. Kaplan–Meier analysis showed that decreased expression of *RUNX3* mRNA was significantly correlated with poor survival rate ($P = 0.016$, Figure 1c). In addition, the possible

[1]Division of Biochemistry and Innovative Cancer Therapeutics, Chiba Cancer Center Research Institute, Chiba, Japan; [2]Department of Molecular Biology and Oncology, Chiba University Graduate School of Medicine, Chiba, Japan; [3]Department of Thoracic Surgery, Forth Hospital of Hebei Medical University, Hebei, PRC; [4]Department of First Surgery, Forth Hospital of Hebei Medical University, Hebei, PRC and [5]Division of Cancer Genomics, Chiba Cancer Center Research Institute, Chiba, Japan. Correspondence: Dr A Nakagawara, Chiba Cancer Center Research Institute, 666-2 Nitona, Chuo, Chiba 260-8717, Japan.
E-mail: akiranak@chiba-cc.jp
Received 10 February 2013; revised 24 April 2013; accepted 3 May 2013; published online 15 July 2013

relationship between *RUNX3* expression levels and various clinical and biological features from these samples were examined and summarized in Supplementary Table 1. Significantly high levels of *RUNX3* expression were found in the low-risk tumors (stages 1, 2 and 4s, $P<0.001$). Statistical correlation was also detectable between *RUNX3* expression and the copy number of *MYCN* ($P=0.047$). The log-rank test demonstrated that several prognostic factors, including *RUNX3*, were significantly correlated with

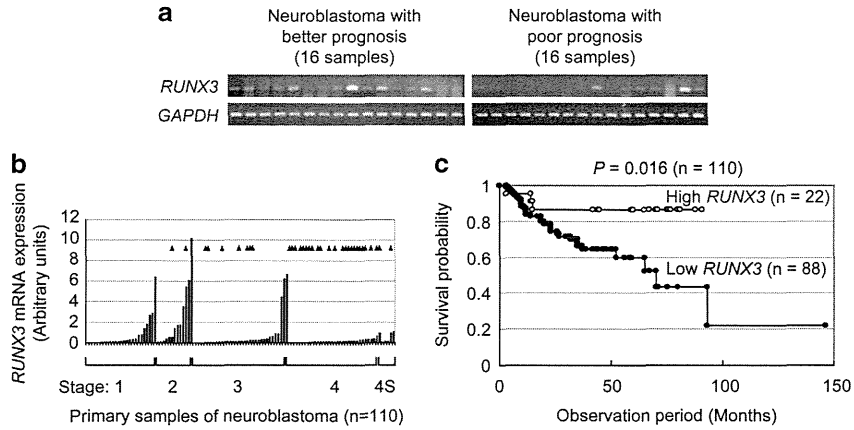

Figure 1. Expression levels of *RUNX3* in primary neuroblastomas. (**a**) Semi-quantitative RT–PCR analysis. Total RNA was prepared from primary samples with better prognosis (stages 1 and 2, *MYCN* single copy, $n=16$) and those with poor prognosis (stages 3 and 4, *MYCN* amplified, $n=16$). RT–PCR was performed to examine the expression levels of RUNX3. Glyceraldehyde 3-phosphate dehydrogenase (GAPDH) is employed for loading control. (**b**) Quantitative real-time PCR analysis. The relative expression levels of *RUNX3* in primary samples (stage 1, 2, 3, 4, and 4S) are shown. *RUNX3* levels were standardized using the corresponding *GAPDH* value of each neuroblastoma sample. Filled triangles indicate fatal cases due to neuroblastoma cancer. (**c**) Kaplan–Meier survival curves of patients with neuroblastoma. Expression levels of *RUNX3* in 110 primary neuroblastoma samples determined by real-time PCR were classified into two categories, such as high (open circle, $n=22$) and low (filled circle, $n=88$) expression groups, based on the mean value of *RUNX3* expression levels.

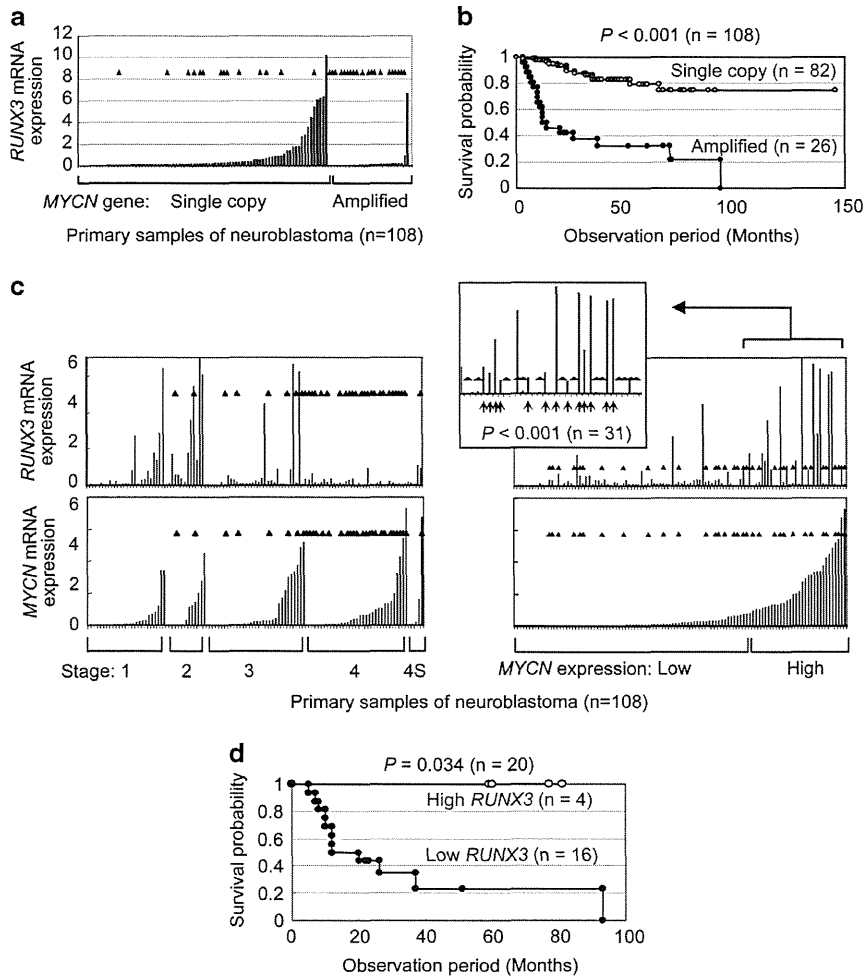

clinical outcome in these 110 neuroblastoma patients (Supplementary Table 2). The multivariate Cox regression analysis showed that *RUNX3* mRNA expression levels are not significantly associated with patient's survival only when International Neuroblastoma Staging System stages or *MYCN* copy number is employed (models C and E in Supplementary Table 3), suggesting that *RUNX3* expression levels are associated with these two factors in terms of patients' survivals.

The relationship between chromosomal deletion at 1p36 and expression of *RUNX3*

As low expression of *RUNX3* is correlated with poor patient's outcome, we sought to identify the possible mechanism underlying the suppression of *RUNX3* expression. According to the data obtained from array-comparative genomic hybridization analysis using UCSF BAC array (2464 BACs, ~1 Mb resolution), among 59 samples that were identified as diploid tumors, 12 tumors revealed to have a partial deletion at chromosome 1p36 (Supplementary Table 4), indicating that *RUNX3* expression is significantly lower in the tumor cells with 1p36 loss than those without the loss. These results suggest that the gene dosage effect is one of the reasons why *RUNX3* expression is decreased in aggressive neuroblastomas.

The outcome relationship between *RUNX3* and *MYCN* expressions in neuroblastoma patients

As we mentioned above, amplification of *MYCN* was significantly associated with low expression of *RUNX3*. A real-time PCR assay quantitatively measuring the expression levels of *RUNX3* also supported this notion (Figure 2a), as a majority of *RUNX3* high expression cases was observed in the tumors with single copy of *MYCN*. Consistent with previous literatures,[28] amplified *MYCN* is apparently related to fatal cases indicated by filled triangles in Figure 2a. Indeed, the Kaplan–Meier survival plot clearly demonstrated that the patients with amplified copies of *MYCN* die more quickly than those with a single copy (Figure 2b). These results lead us to the hypothesis that amplified copies of *MYCN* gene induce higher level of *MYCN* mRNA expression and high MYC pathway activity, resulted in death of neuroblastoma patients in which *RUNX3* is expressed in a low level. To test this possibility, the expression levels of *MYCN* in the primary neuroblastoma samples were quantitatively measured by a real-time PCR and were compared with *RUNX3* levels (Figure 2c). Nearly all tumors in stage 4 were fatal cases (shown by filled triangles in Figure 2c) and were associated with higher *MYCN* and lower *RUNX3* expressions (Figure 2c, left panels). In contrast, survivals were enriched in lower International Neuroblastoma Staging System stages (1 and 2) and were generally accompanied by lower *MYCN* and higher *RUNX3* expressions. Next, the primary neuroblastoma samples were arranged according to the expression levels of *MYCN* to further elucidate the correlation between *MYCN* and *RUNX3* expressions (Figure 2c, right panels). Primary samples were classified into two groups using the mean value of MYCN as the cutoff value. We found that, among the *MYCN* high-expression group, patients with higher expression levels of *RUNX3* tend to survive, whereas those with low expression died (Figure 2c, inset in right panels). Kaplan–Meier plot of the primary samples in which *MYCN* is highly expressed also supports this notion (Figure 2d). This result suggests that *RUNX3* high expression is closely associated with survival possibility of neuroblastoma patients, even though some of them expressed high level of *MYCN*.

The biological function of RUNX3 in neuroblastoma cells

The clinical study above promoted us to further investigate the function of RUNX3 in neuroblastoma cell lines. SK-N-BE

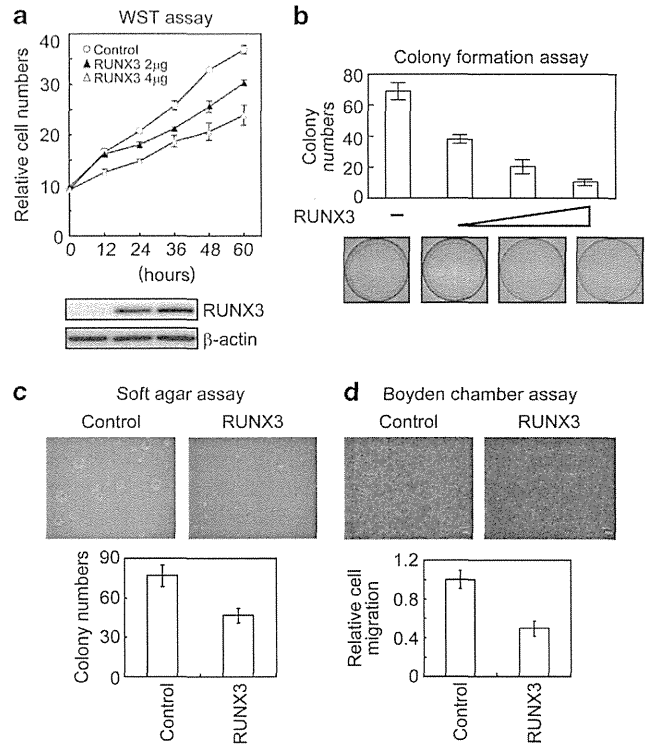

Figure 3. Transient transfection of RUNX3 suppresses the growth and migration of neuroblastoma cells. (**a**) WST assay. Empty vector or increasing amounts of RUNX3 expression plasmid were transfected into SK-N-BE cells. Cell growth was measured at indicated hours. The expression of exogenous RUNX3 was shown by immunoblotting (bottom panels). (**b**) Colony formation assay. SK-N-BE cells were transfected with increasing amounts of RUNX3 expression plasmid (0.5, 1 and 2 μg). Total amounts of plasmid DNA per transfection were kept constant (2 μg) with empty vector. The histograms represent the number of colonies in each group. Representative colony formation images are also shown. (**c**) Soft agar assay. SK-N-BE cells were transfected by either mock or RUNX3-expression vector. The cells were seeded onto soft agar plates in triplicate. The histograms represent the number of colonies (diameters >300 μm) in each plate. Representative colony images are also shown. (**d**) Boyden chamber assay. Empty vector or RUNX3 expression plasmid was transfected into SK-N-BE cells. Numbers of migrated cells were counted and are represented as relative values. Control group was set to 1. Error bars represent the standard deviation obtained from triplicate experiments.

Figure 2. Inverse correlation between *RUNX3* and *MYCN* expression. Filled triangles shown in each panel indicate fatal cases due to neuroblastoma cancer. (**a**) Quantitative real-time PCR of *RUNX3* expression. Primary samples are classified into two groups based on the copy number of *MYCN* gene (single copy or amplified). (**b**) Kaplan–Meier survival plot according to a copy number of *MYCN*. A total of 108 primary neuroblastomas were classified into two categories (single or amplified). (**c**) The expression levels of *RUNX3* (top panels) and *MYCN* (bottom panels). Primary neuroblastoma samples are arranged according to stages (left panels) or relative *MYCN* expression values (right panels). *RUNX3* expression levels associated with high expression levels of *MYCN* are shown in detail (inset). Arrowheads indicate the survivals in which both *RUNX3* and *MYCN* were highly expressed. (**d**) Kaplan–Meier survival plot according to *RUNX3* expression levels. Twenty primary neuroblastomas in which *MYCN* is highly expressed were classified into two categories, such as high (open circle, $n=4$) and low (filled circle, $n=16$) *RUNX3* expression groups, based on the mean value of *RUNX3* expression levels.

(*MYCN* amplified) cells were transiently transfected with empty vector or increasing amounts of RUNX3 expression vector and the cell growth was examined by WST (water soluble tetrazolium salts) assay and colony formation assay. RUNX3 overexpression decreased the growth rate in a dose-dependent manner (Figure 3a). Similar results were obtained by conventional colony formation assay (Figure 3b). Furthermore, colony formation assay utilizing soft agar demonstrated that overexpression of RUNX3 decreased anchorage-independent cell growth, suggesting that RUNX3 could inhibit the oncogenic property of neuroblastoma-derived cell line (Figure 3c). In order to better understand the changes in the cellular phenotype mediated by RUNX3, we tested whether RUNX3 had any role in regulating the cell migration of neuroblastoma. Toward this, Boyden chamber migration assay was performed. Overexpression of RUNX3 decreased the number of cells that migrate to the lower side of the membrane, whereas the transfection of an empty vector did not (Figure 3d). This result indicates that RUNX3 inhibits the migration activity of neuroblastoma-derived cell line.

RUNX3 overexpression reduces MYCN expression at protein level in neuroblastoma cells

As there was a close correlation between high expression of *RUNX3* and favourable outcome in neuroblastoma patients in which *MYCN* is highly expressed, we hypothesized that RUNX3 may negatively regulate *MYCN* oncogenic activities, resulting in survival of neuroblastoma patients. Thus, we examined whether RUNX3 could control MYCN expression at either mRNA or protein level. Overexpression of RUNX3 decreased the MYCN proteins in a dose- and time-dependent manner (Figure 4a, left panels and Figure 4b), whereas RT–PCR showed that the mRNA expression level of *MYCN* was not affected by the exogenous *RUNX3* overexpression (Figure 4a, right panels). Essentially, similar results were obtained utilizing another *MYCN*-amplified neuroblastoma cell line NLF. These data indicate that RUNX3 reduced the expression of MYCN at protein level rather than mRNA level, suggesting that RUNX3 negatively regulates MYCN expression by the post-translational mechanism. Immunofluorescence microscopy demonstrated that the cells in which exogenous RUNX3 (red) was overexpressed showed less degree of endogenous MYCN (green; Figure 4c, top panels), indicating that exogenous RUNX3 and endogenous MYCN are mutually exclusive in terms of the protein expression pattern. We further examined the number of cells that have different expression patterns of RUNX3 and MYCN. Majority of the cells show either MYCN or RUNX3 expressions, and less than 10% of cells express both or none (Figure 4c, bottom panel). These results demonstrated that, at protein level, MYCN is inversely correlated with RUNX3 expression. In order to investigate reduction of MYCN protein in detail, the

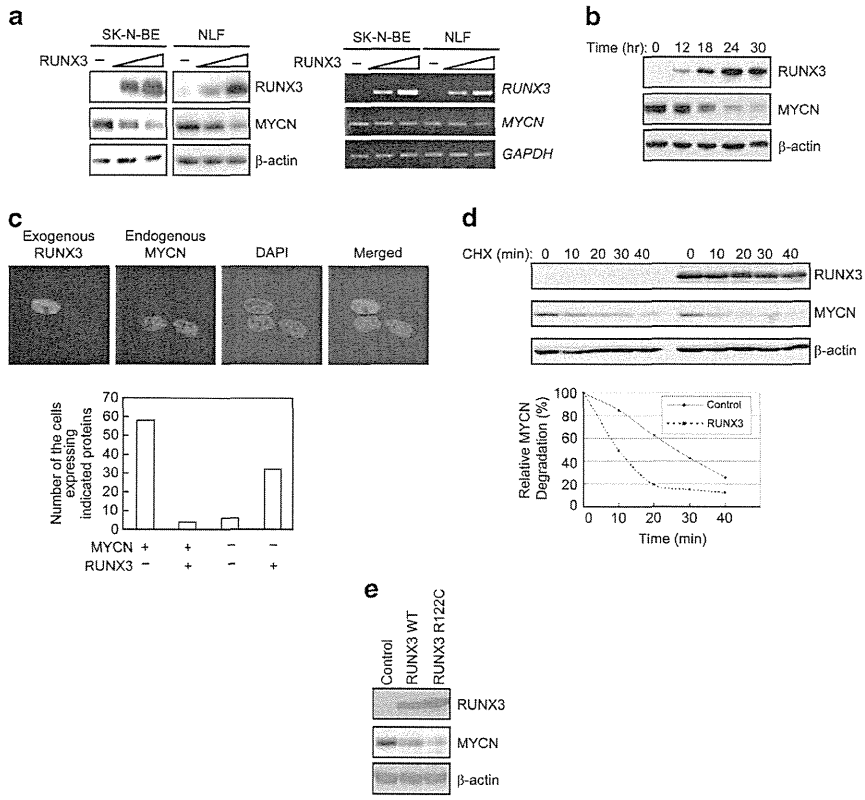

Figure 4. RUNX3 overexpression reduces the protein level of MYCN in neuroblastoma cells. (**a**) RUNX3 inhibits MYCN expression at protein level. SK-N-BE and NLF cells were transfected with empty vector or increasing amounts of RUNX3-expressing plasmid. Whole-cell lysates and total RNA were subjected to immunoblotting (IB; left panels) or RT–PCR (right panels), respectively. Actin and *GAPDH* were used as loading controls. (**b**) Time course. SK-N-BE cells were transfected with RUNX3-expressing plasmid. Cell lysates were prepared at indicated time points and were subjected to IB. (**c**) The subcellular localization of RUNX3 and MYCN are detected by immunofluorescent staining in SK-N-BE cells. Exogenous RUNX3 and endogenous MYCN were stained by anti-MYC tag (red) or anti-MYCN (green) antibodies, respectively. Nucleus was visualized by 4′-6-diamidino-2-phenylindole (DAPI) staining. The histogram represents the number of cells expressing indicated genes ($n = 100$). (**d**) RUNX3 decreases the half-life of MYCN. Empty vector or RUNX3-expressing plasmid was transfected into SK-N-BE cells, and the cells were treated with cycloheximide (CHX) and harvested at the indicated time points. A measure of 40 μg (the cells transfected with empty vector) or 60 μg (the cells with RUNX3 expression vector) of the cell lysate was employed, respectively. (**e**) MYCN degradation mediated by wild-type RUNX3 and transcriptionally deficient mutant RUNX3-R122C. SK-N-BE cells were transfected with empty vector, RUNX3 or point-mutated RUNX3-R122C-expressing plasmid.

degradation rate of endogenous MYCN in the absence or presence of RUNX3 was compared. Cycloheximide was used to inhibit the synthesis of new MYCN protein. Immunoblotting showed that the degradation of MYCN was accelerated by RUNX3 (Figure 4d), suggesting a negative regulation of RUNX3 on MYCN stability. As RUNX3 is a transcription factor, degradation of MYCN may be a secondary effect of the transcriptional activation mediated by RUNX3. To exclude out this possibility, we employed RUNX3-R122C, a transcriptionally incompetent mutant of RUNX3,[29,30] to test whether the transcriptional activity of RUNX3 is essential or not for the degradation of MYCN. Both RUNX3 wild type and RUNX3-R122C were able to facilitate the degradation of MYCN (Figure 4e), suggesting that the transcriptional activity of RUNX3 is not necessary. Therefore, we conclude that the protein degradation of MYCN is directly mediated by RUNX3.

RUNX3 promotes ubiquitination of MYCN, resulting in MYCN degradation

The protein stability of MYCN is regulated by a complex signaling network and the degradation of MYCN is mainly promoted by an ubiquitin-proteasome pathway.[31–33] Thus, we investigated the protein stability of MYCN in the presence or absence of proteasome inhibitor MG132. Immunoblotting showed that the overexpression of RUNX3 decreased endogenous MYCN in a dose-dependent manner, and this decrease was inhibited by an MG132 treatment (Figure 5a, left panel). This result suggests that destabilization of MYCN mediated by RUNX3 depends on the proteasomal function. Similar results were obtained in another neuroblastoma cell line NLF (Figure 5a, right panel). As the MYCN proteolysis occurs through the proteasome pathway, we asked whether ubiquitination is involved in this process. In the presence of MG132, RUNX3 efficiently facilitated the polyubiquitination of MYCN (Figure 5b, top panel). Similarly, increasing polyubiquitination of MYCN was detected in the cell lysate immunoprecipitated by anti-MYCN antibody followed by immunoblotting with anti-ubiquitin antibody (Figure 5b, bottom panel). Taken together, these results suggest that RUNX3 destabilizes MYCN through the ubiquitin-proteasome pathway.

Physical interaction between RUNX3 and MYCN

As shown above, the transcriptionally deficient mutant RUNX3-R122C can also induce the degradation of MYCN as efficiently as wild-type RUNX3, suggesting that the transcriptional activity of RUNX3 is unnecessary in this process. Therefore, we speculated that RUNX3 may directly interact with MYCN to induce its degradation. To confirm this postulation, first we examined the potential interaction between exogenous RUNX3 and MYCN. HeLa cells were transiently co-transfected with expression plasmids of MYC-tagged RUNX3 (RUNX3-MYC) and HA-tagged MYCN (HA-MYCN). Anti-MYC tag antibody precipitated RUNX3-MYC and HA-MYCN. As well, anti-HA tag antibody precipitated HA-MYCN and RUNX3-MYC, confirming that RUNX3 and MYCN could interact with each other. Furthermore, the interaction between endogenous proteins was confirmed in SK-N-BE cells (Figure 6b). As RUNX3-R122C induces the destabilization of MYCN, we also investigated whether RUNX3-R122C could bind to MYCN. We found that RUNX3-R122C co-immunoprecipitated with endogenous MYCN (Figure 6c), suggesting that the interaction between RUNX3 and MYCN is important in the process of MYCN degradation. To identify the regions of RUNX3 required for the interaction with MYCN, *in vitro* translation-coupled pulldown assay was performed (Figure 6d). Plasmids expressing a series of deletion mutants of RUNX3 protein were tranfected into HEK293 cells. Radiolabeled MYCN bound to the full length as well as several deletion constructs containing intact runt domain (deletion constructs 249, 200, Δ1-33 and Δ1-66). However, deletion constructs containing partial runt domain (Δ1-100, Δ1-133 and

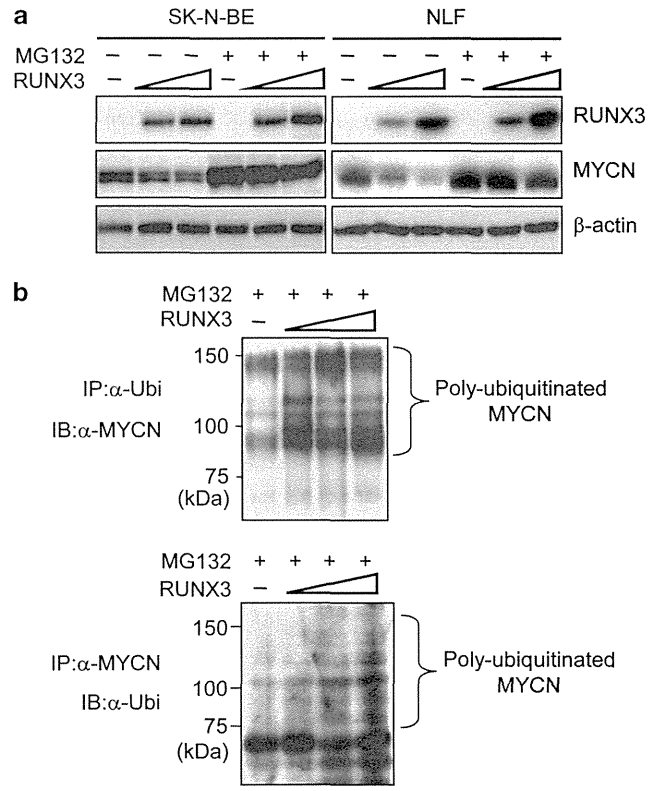

Figure 5. RUNX3 promotes ubiquitination of MYCN, resulting in MYCN degradation. (**a**) RUNX3-mediated MYCN degradation depends on proteasome function. Increasing amounts of RUNX3 expression plasmid (0, 2 and 4 μg) were transfected into SK-N-BE or NLF cells. MG132 (20 μM) was added to block proteasomal degradation. (**b**) RUNX3 induces poly-ubiquitination of MYCN. Increasing amounts of RUNX3 expression plasmid were transfected into SK-N-BE cells. Cells were treated with MG132. Whole-cell lysates were immunoprecipitated with anti-ubiquitin antibody and analyzed by immunoblotting with anti-MYCN antibody (top panel). The same cell lysates were immunoprecipitated with anti-MYCN antibody and analyzed by immunoblotting with anti-ubiquitin antibody (bottom panel). IP, immunoprecipitation; IB, immunoblotting.

Δ1-166) failed to bind to MYCN, suggesting that the N-terminal side of the runt domain is responsible for MYCN–RUNX3 interaction. Interestingly, a deletion construct fully lacking the runt domain (Δ1-200) retained the interaction capability. It was assumed that transactivation domain is also capable of MYCN interaction and the C-terminal side of the runt domain interferes it. When RUNX3-MYC and HA-MYCN were co-overexpressed, we observed colocalization of these exogenous proteins in the nucleus after 24 h of transfection, further supporting our notion (Figure 6e). Taken together, these results suggest that RUNX3 and MYCN physically interact through the runt domain of RUNX3.

RUNX3 suppresses the expression of MYCN target genes

Considering the degradation of MYCN acting as a transcription factor in neuroblastoma,[31,34] we predicted that RUNX3 may also inhibit the expression of genes targeted by MYCN. To confirm this, SK-N-BE cells were transfected with increasing amounts of RUNX3 expression plasmid. RT–PCR demonstrated that the expression levels of mRNA of MYCN-target genes, such as *MDM2*, *ID2* and *P53*,[35–37] were decreased, whereas mRNA of endogenous *MYCN* was not affected (Figure 7a). As well, overexpression of RUNX3 could overcome even exogenous MYCN to suppress the target

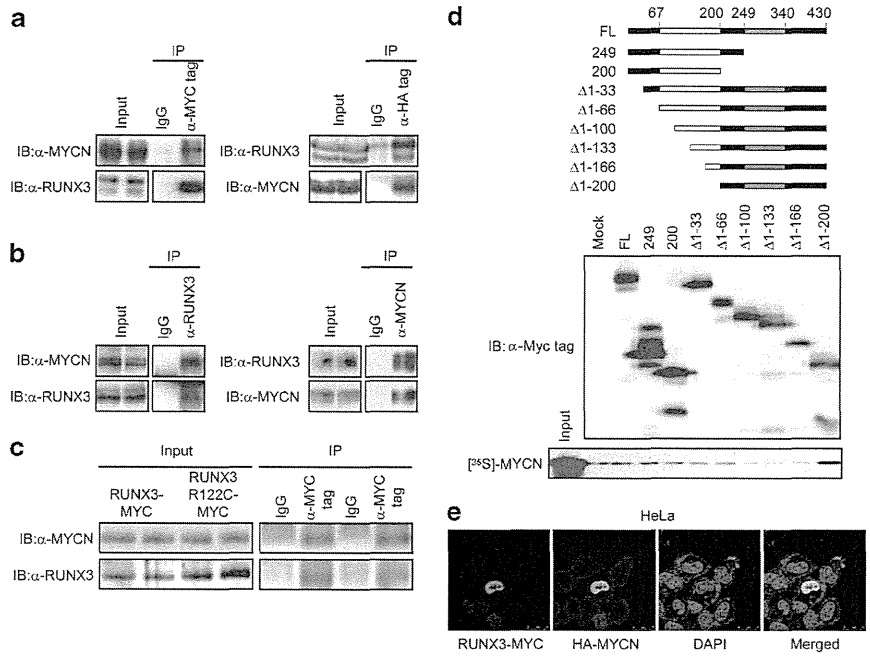

Figure 6. Physical interaction between RUNX3 and MYCN. (**a**) Exogenous MYCN and RUNX3 interact in HeLa cells. HA-tagged MYCN was co-expressed with MYC-tagged RUNX3 in HeLa cells. Cells were treated with MG132 to inhibit the MYCN degradation. Cell lysates were immunoprecipitated with mouse IgG or anti-HA tag antibody and immunoblotted with anti-MYCN antibody and anti-RUNX3 antibody (left panels). The cell lysates were immunoprecipitated with mouse IgG or anti-MYC tag antibody and immunoblotted with anti-RUNX3 antibody and anti-MYCN antibody (right panels). (**b**) Interaction between endogenous RUNX3 and MYCN. SK-N-BE cells were treated with MG132. Whole-cell lysates were subjected to immunoprecipitation with anti-RUNX3 antibody (left panels) or anti-MYCN antibody (right panels), followed by immunoblotting with anti-MYCN and anti-RUNX3 antibody, respectively. (**c**) Both RUNX3 and RUNX3-R122C interact with endogenous MYCN in SK-N-BE cells. MYC-tagged RUNX3 and MYC-tagged RUNX3-R122C expression plasmids were transfected into SK-N-BE cells. After MG132 treatment, whole-cell lysates were subjected to immunoprecipitation with anti-MYC tag antibody followed by immunoblotting with anti-MYCN and anti-RUNX3 antibody. (**d**) *In vitro* translation-coupled pulldown assay. The schematic diagram (top panel) represents full length (FL) and a series of deletion constructs of RUNX3. Runt domain (open box) and transactivation domain (shaded box) are indicated. Overexpression of FL and deletion mutants of RUNX3 in HEK293 cells were confirmed by anti-Myc tag antibody on western blotting (middle panel). ^{35}S-labeled MYCN pulled down by these RUNX3 constructs were detected by autoradiography (bottom panel). (**e**) Co-localization of RUNX3 and MYCN in the nucleus by immunofluorescent staining. HeLa cells were transfected with MYC-tagged RUNX3 (1 μg) and HA-tagged MYCN (4 μg), and were incubated with MG132. Each nucleus was visualized by 4′-6-diamidino-2-phenylindole (DAPI) staining. Exogenous RUNX3 and MYCN were detected in the nucleus by anti-MYC tag (red) and anti-HA tag (green) antibodies. Proteosome inhibitor MG132 was employed to inhibit MYCN degradation when RUNX3 was overexpressed. IP, immunoprecipitation; IB, immunoblotting.

genes (*MDM2*, *ODC1* and *CAD*) in HeLa cells (Figure 7b). Finally, we employed a couple of deletion mutants of RUNX3 (Figure 6d) to confirm the notion above. RUNX3 full length and Δ1-66 induced protein degradation of MYCN as well as suppression of MYCN-target genes, MDM2 and CAD (Figure 7c). However, unbound mutants (Δ1-100 and Δ1-200) induced neither MYCN degradation nor gene suppression. It should be noted that one of the deletion mutants (200) also failed to induce degradation and suppression, while it still binds to MYCN (Figure 6d). The deletion mutant 200 is the C-terminally truncated form of RUNX3 completely lacking the transactivation domain. As previous literatures demonstrated that this form of truncated RUNX3 lost tumor suppression capability,[38,39] we assume that this deletion mutant cannot recruit additional factors required for the MYCN degradation, even though it can interact with MYCN *in vitro*. These results clearly demonstrated that RUNX3 inhibits transcriptional activation of MYCN-target genes, suggesting that RUNX3 can block the oncogenic signaling pathway mediated by MYCN.

DISCUSSION

In this study, we found that *RUNX3* could overcome oncogenic behavior of MYCN. Consistent with our findings, *RUNX3* induces the degradation of estrogen receptor α and acts as a tumor suppressor in breast cancer.[15] Thus, we conclude that RUNX3 destabilizes oncogenic proteins, such as estrogen receptor α and MYCN, to exert its tumor-suppressive function.

Threonine 50 (T50) and serine 54 (S54) are critical amino-acid residues responsible for instability of MYCN. Initial monophosphorylation at S54 by cyclin B/cdk1 stabilizes MYCN, and primes MYCN for a second phosphorylation at T50 controlled by glycogen synthase kinase 3β. MYCN protein monophosphorylated at T50 binds to E3 ligase Fbxw7 followed by ubiquitination and degradation.[31–33,40] Early report suggested that RUNX3 transcriptionally inhibits Akt expression and therefore promotes glycogen synthase kinase 3β activation in the gastric cancer cell lines.[17] However, we did not detect the induction of glycogen synthase kinase 3β expression by RUNX3 in neuroblastoma cell line (data not shown). Rather, we showed that the transcriptionally incompetent mutant of RUNX3 could induce the degradation of MYCN, suggesting that the transcriptional activity of RUNX3 is not essential for MYCN degradation. Considering the interaction between RUNX3 and MYCN, it is possible that RUNX3 might recruit an E3 ubiquitin ligase and forms a protein complex to induce the degradation of MYCN, resulting in suppression of the transcriptional targets of MYCN. These results explain the molecular mechanism of higher survival rate observed in neuroblastoma patients in whom both *MYCN* and *RUNX3* are highly expressed. We hypothesized that high

expression of RUNX3 induces the proteasome-mediated degradation of MYCN and inhibits the MYCN oncogenic function, which contributes to the favorable outcome. In addition, as we demonstrated by cellular migration and soft agar assay, RUNX3 overexpression reduced the cellular mobility as well as anchorage-independent cell growth. As these are typical indicators of the tumor-specific property of the cell lines, it was assumed that RUNX3 overexpression improves the survival rate of the patients by inhibiting the oncogenic properties of the tumor cells.

RUNX3 is located at 1p36 where nearly 30% of neuroblastoma cases had a deletion.[3–5] Consistently, we found a positive correlation between low expression of *RUNX3* and the 1p36 loss. Although it has been reported that *RUNX3* is inactivated by hypermethylation at its promoter region in various cancers,[12–14] we did not find statistically significant correlation between the methylation status and mRNA expression levels of *RUNX3* in 110 primary neuroblastoma samples (data not shown). RUNX3 transcription factor has pivotal roles in neural development and, as far as we examined, *RUNX3* expression is very low in the majority of neuroblastoma cell lines available. Therefore, we mainly employed overexpression system, rather than knockdown strategy of *RUNX3*. Such low level of *RUNX3* could be necessary to establish the neuroblastoma cell line in which *MYCN* gene is amplified. We further assume that chromosomal 1p deletion is one of the major reasons responsible for the low *RUNX3* expression in both primary tumors and cell lines of neuroblastoma.

Taken together, we demonstrated that *RUNX3* acts as a tumor-suppressor gene in neuroblastoma. Activation of RUNX3 may suppress MYCN-mediated downstream signaling pathway. We therefore believe that the analysis of RUNX3 expression are useful for identifying low-risk neuroblastoma that are initially diagnosed as high risk and mostly increase the prognostic sensitivity.

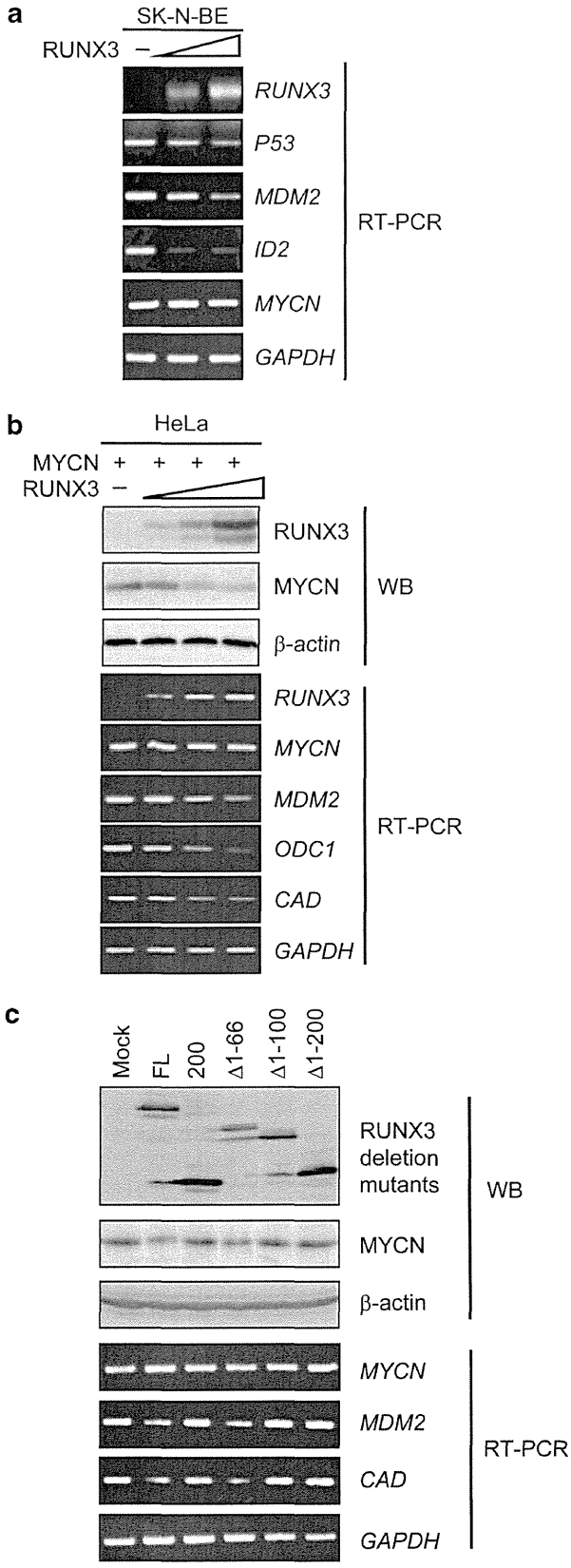

MATERIALS AND METHODS

Clinical specimens

Tumor DNA and RNA samples were obtained from 110 tumor specimens in our Neuroblastoma Resource Bank at Chiba Cancer Center Research Institute. The specimens were kindly provided from various institutions and hospitals where informed consent was obtained. All tumors were diagnosed clinically as well as pathologically as neuroblastoma and staged according to the International Neuroblastoma Staging System criteria. *MYCN* copy number, *TRKA* mRNA expression levels and DNA index were measured as reported previously.[24]

Reverse transcription–PCR and real-time PCR analyses

Total RNA was prepared from the primary neuroblastoma tissues and cell lines, followed by the first strand synthesis. RT–PCR was performed according to the manufacturer's instructions (Invitrogen, Carlsbad, CA, USA). Quantitative real-time PCR was carried out using SYBR GREEN method as the manufacturer described (Applied Biosystems, Foster City, CA, USA). Primer sequences are in the Supplementary Information.

Array-comparative genomic hybridization

Array-comparative genomic hybridization analysis was performed using UCSF BAC array (2464 BACs with 1 Mb resolution (average)) and 59 primary neuroblastomas identified as diploid were subjected to further analysis.

Figure 7. RUNX3 suppresses the expression of genes targeted by MYCN. (**a**) RUNX3 inhibits the expression of MYCN-target genes. SK-N-BE cells were transfected with RUNX3-expressing plasmid. Total RNA was used for RT–PCR. (**b**) RUNX3 inhibits the transactivation ability of exogenous MYCN. HeLa cells were co-transfected with indicated combinations of expression plasmids. Whole-cell lysates and total RNA were subjected to immunoblotting (IB; upper panels) or RT–PCR (lower panels), respectively. Actin and *GAPDH* were used as loading controls. (**c**) Unbound mutants of RUNX3 failed to induce MYCN degradation and transcriptional activation of MYCN target genes. SK-N-BE cells were transfected with indicated expression plasmids. Whole-cell lysates and total RNA were subjected to IB (upper panels) or RT–PCR (lower panels), respectively. FL, full length; WB, western blotting.

Experimental procedures and the criteria for losses and gains were described previously.[24,41]

Cell culture and transfection

The human neuroblastoma cell lines (SK-N-BE, NLF) were maintained in RPMI 1640 medium (Nissui, Tokyo, Japan) supplemented with 10% heat-inactivated fetal bovine serum (Invitrogen) and 100 mg/ml of penicillin-streptomycin (Invitrogen). HeLa and HEK293 cells were cultivated in Dulbecco's modified Eagle's medium supplemented with 10% heat-inactivated fetal bovine serum (Invitrogen) and antibiotic mixture. Transient transfection was performed using Lipofectmine 2000 transfection reagent (Invitrogen) according to the manufacturer's instructions.

Immunoblotting, immunoprecipitation and *in vitro* translation-coupled pulldown assay

For immunoblotting, cells were lysed in a lysis buffer containing 25 mM Tris-HCl, pH 7.5, 137 mM NaCl, 2.7 mM KCl, 1%Triton X-100 and protease inhibitor mixture (Sigma, St Louis, MO, USA), and spun to separate insoluble debris from the clear lysates. Equal amounts of cell lysates were separated by SDS–polyacrylamide gel electrophoresis and transferred onto Immobilon-P membranes (Milipore, Bedford, MA, USA). The transferred membranes were incubated with monoclonal anti-MYC tag (9B11, Cell Signaling Technology, Beverly, MA, USA), polyclonal anti-HA tag (561-5, MBL, Woburn, MA, USA), monoclonal anti-MYCN (Ab-1, Oncogene Research Products, Cambridge, MA, USA), polyclonal anti-MYCN (9405, Cell Signaling), polyclonal anti-actin (20–33, Sigma), monoclonal anti-RUNX3 (R3-5G4, Abcam, Cambridge, UK), monoclonal anti-ubiquitin (FK-2, Enzo, Farmingdale, NY, USA) antibodies, followed by incubation with the appropriate horseradish peroxidase-conjugated secondary antibodies (Cell Signaling Technology). For immunoprecipitation, the cell lysate of each sample contains total weight of approximately 600 μg of the protein that was extracted from 2×10^7 cells. The cell lysates were precleared with 30 μl of protein G-Sepharose suspension (Amersham Biosciences AB, Corston, UK) and then incubated with anti-MYCN monoclonal antibody or anti-RUNX3 monoclonal antibody for 2 h at 4 °C. For *in vitro* translation-coupled pulldown assay, full-length or deletion constructs of MYC-tagged RUNX3 were transfected into HEK293 cells and the cell lysate was pre-purified by MYC-tag antibody and protein G-Sepharose beads. [^{35}S] Methionine-labeled MYCN was generated in the coupled transcription/translation system (Promega, Madison, WI, USA) and mixed with pre-purified RUNX3 proteins for 2 h at 4 °C. After purification, ^{35}S-labeled bound proteins were analyzed by 10% SDS–polyacrylamide gel electrophoresis and visualized by autoradiography.

Immunofluorescence analysis

For immunofluorescence, SK-N-BE and HeLa cells were grown on coverslips and transfected with indicated expression plasmids. Forty-eight hours after transfection, cells were fixed in 100% methanol for 20 min at −20 °C, blocked in 3% bovine serum albumin, stained with the corresponding antibodies, and examined with a laser scanning confocal microscope.

Protein stability and ubiquitination assay

Cells were harvested at different time points after pretreatment with cycloheximide (100 μg/ml), and the cell lysates were employed for immunoblotting. For ubiquitination assay, SK-N-BE cells were transfected with or without RUNX3. SK-N-BE cells were exposed to the proteasomal inhibitor MG132 (20 μM) for 6 h before harvest. Cell lysates were incubated with anti-MYCN or anti-ubiquitin monoclonal antibody.

Boyden chamber assay

For the Boyden chamber assay, 50 000 pre-transfected cells were resuspended in serum-free medium and plated in the top chamber of Transwell inserts (Falcon, San Jose, CA, USA). After 24 h of transfection, cells on the bottom surface of the insert were fixed in 10% formalin and stained with a crystal violet solution. Results shown are representative of three independent experiments.

Cell proliferation assay

Pre-transfected neuroblastoma cells were seeded in 96-well plates at a density of 10^3 cells per well in a final volume of 100 μl. WST assay was performed according to the manufacturer's instruction (Cell counting Kit-8; DOJINDO, Kumamoto, Japan).

Colony formation assay

SK-N-BE cells were seeded at a final density of 500 000 cells/6 cm plate and allowed to attach overnight. Total amount of plasmid DNA per transfection was kept constant (2 μg) with pcDNA3. Forty-eight hours after transfection, cells were transferred to the fresh medium containing G418 (400 μg/ml). After 14 days, viable colonies were washed in phosphate-buffered saline and stained with Giemsa solution. For colony formation assay utilizing soft agar,[42] 2.5×10^3 cells of the RUNX3 transfected or mock transfected were seeded in triplicate in 35-mm cell culture plates containing 0.2% agar and RPMI 1640 supplemented with 10% fetal bovine serum. After 20 days, colonies with diameters >300 μm were scored as positive.

Construction of a series of deletion mutants and a point mutant of RUNX3

RUNX3 deletion mutants were amplified by PCR. PCR primers including *Eco*RI and *BamH*I restriction sites (Supplementary Information) and the amplicons were subcloned into pcDNA3.1. The point mutated RUNX3-R122C was generated utilizing the QuikChange II XL site-directed mutagenesis kit (Agilent Technologies, Loveland, CO, USA). The PCR fragments to construct these expression plasmids were verified by DNA sequencing.

CONFLICT OF INTEREST

The authors declare no conflict of interest.

ACKNOWLEDGEMENTS

This work was supported in part by a Grant-in-Aid from the Ministry of Health, Labour and Welfare for Third Term Comprehensive Control Research for Cancer, JSPS KAKENHI (Grant number 24249061) and a Grant from Takeda Science Foundation.

REFERENCES

1 Park JR, Eggert A, Caron H. Neuroblastoma: biology, prognosis, and treatment. *Hematol Oncol Clin North Am* 2010; **24**: 65–86.
2 Nakagawara A. Neural crest development and neuroblastoma: the genetic and biological link. *Prog Brain Res* 2004; **146**: 233–242.
3 Cotterill SJ, Pearson AD, Pritchard J, Foot AB, Roald B, Kohler JA *et al.* Clinical prognostic factors in 1277 patients with neuroblastoma: results of The European Neuroblastoma Study Group 'Survey' 1982-1992. *Eur J Cancer* 2000; **36**: 901–908.
4 Maris JM, Hogarty MD, Bagatell R, Cohn SL. Neuroblastoma. *Lancet* 2007; **369**: 2106–2120.
5 Ohira M, Oba S, Nakamura Y, Isogai E, Kaneko S, Nakagawa A *et al.* Expression profiling using a tumor-specific cDNA microarray predicts the prognosis of intermediate risk neuroblastomas. *Cancer Cell* 2005; **7**: 337–350.
6 Riley RD, Heney D, Jones DR, Sutton AJ, Lambert PC, Abrams KR *et al.* A systematic review of molecular and biological tumor markers in neuroblastoma. *Clin Cancer Res* 2004; **10**: 4–12.
7 Seeger RC, Brodeur GM, Sather H, Dalton A, Siegel SE, Wong KY *et al.* Association of multiple copies of the N-myc oncogene with rapid progression of neuroblastomas. *N Engl J Med* 1985; **313**: 1111–1116.
8 Suenaga Y, Kaneko Y, Matsumoto D, Hossain MS, Ozaki T, Nakagawara A. Positive auto-regulation of MYCN in human neuroblastoma. *Biochem Biophys Res Commun* 2009; **390**: 21–26.
9 Maris JM, Weiss MJ, Guo C, Gerbing RB, Stram DO, White PS *et al.* Loss of heterozygosity at 1p36 independently predicts for disease progression but not decreased overall survival probability in neuroblastoma patients: a Children's Cancer Group study. *J Clin Oncol* 2000; **18**: 1888–1899.
10 White PS, Maris JM, Beltinger C, Sulman E, Marshall HN, Fujimori M *et al.* A region of consistent deletion in neuroblastoma maps within human chromosome 1p36.2-36.3. *Proc Natl Acad Sci USA* 1995; **92**: 5520–5524.
11 Ohira M, Kageyama H, Mihara M, Furuta S, Machida T, Shishikura T *et al.* Identification and characterization of a 500-kb homozygously deleted region at 1p36.2-p36.3 in a neuroblastoma cell line. *Oncogene* 2000; **19**: 4302–4307.
12 Bangsow C, Rubins N, Glusman G, Bernstein Y, Negreanu V, Goldenberg D *et al.* The RUNX3 gene--sequence, structure and regulated expression. *Gene* 2001; **279**: 221–232.
13 Levanon D, Groner Y. Structure and regulated expression of mammalian RUNX genes. *Oncogene* 2004; **23**: 4211–4219.

14 Chuang LS, Ito Y. RUNX3 is multifunctional in carcinogenesis of multiple solid tumors. *Oncogene* 2010; **29**: 2605–2615.
15 Huang B, Qu Z, Ong CW, Tsang YH, Xiao G, Shapiro D *et al.* RUNX3 acts as a tumor suppressor in breast cancer by targeting estrogen receptor alpha. *Oncogene* 2012; **31**: 527–534.
16 Lee CW, Chuang LS, Kimura S, Lai SK, Ong CW, Yan B *et al.* RUNX3 functions as an oncogene in ovarian cancer. *Gynecol Oncol* 2011; **122**: 410–417.
17 Lin FC, Liu YP, Lai CH, Shan YS, Cheng HC, Hsu PI *et al.* RUNX3-mediated transcriptional inhibition of Akt suppresses tumorigenesis of human gastric cancer cells. *Oncogene* 2012; **31**: 4302–4316.
18 Yamada C, Ozaki T, Ando K, Suenaga Y, Inoue K, Ito Y *et al.* RUNX3 modulates DNA damage-mediated phosphorylation of tumor suppressor p53 at Ser-15 and acts as a co-activator for p53. *J Biol Chem* 2010; **285**: 16693–16703.
19 Inoue K, Ito K, Osato M, Lee B, Bae SC, Ito Y. The transcription factor Runx3 represses the neurotrophin receptor TrkB during lineage commitment of dorsal root ganglion neurons. *J Biol Chem* 2007; **282**: 24175–24184.
20 Inoue K, Shiga T, Ito Y. Runx transcription factors in neuronal development. *Neural Dev* 2008; **3**: 20.
21 Nakagawara A, Azar CG, Scavarda NJ, Brodeur GM. Expression and function of TRK-B and BDNF in human neuroblastomas. *Mol Cell Biol* 1994; **14**: 759–767.
22 Nakagawara A. Trk receptor tyrosine kinases: a bridge between cancer and neural development. *Cancer Lett* 2001; **169**: 107–114.
23 Inoue K, Ito Y. Neuroblastoma cell proliferation is sensitive to changes in levels of RUNX1 and RUNX3 protein. *Gene* 2011; **487**: 151–155.
24 Ohira M, Morohashi A, Inuzuka H, Shishikura T, Kawamoto T, Kageyama H *et al.* Expression profiling and characterization of 4200 genes cloned from primary neuroblastomas: identification of 305 genes differentially expressed between favorable and unfavorable subsets. *Oncogene* 2003; **22**: 5525–5536.
25 Nakagawara A, Arima M, Azar CG, Scavarda NJ, Brodeur GM. Inverse relationship between trk expression and N-myc amplification in human neuroblastomas. *Cancer Res* 1992; **52**: 1364–1368.
26 Nakagawara A. Molecular basis of spontaneous regression of neuroblastoma: role of neurotrophic signals and genetic abnormalities. *Hum Cell* 1998; **11**: 115–124.
27 Akter J, Takatori A, Hossain MS, Ozaki T, Nakazawa A, Ohira M *et al.* Expression of NLRR3 orphan receptor gene is negatively regulated by MYCN and Miz-1, and its downregulation is associated with unfavorable outcome in neuroblastoma. *Clin Cancer Res* 2011; **17**: 6681–6692.
28 Westermann F, Schwab M. Genetic parameters of neuroblastomas. *Cancer Lett* 2002; **184**: 127–147.
29 Chi XZ, Yang JO, Lee KY, Ito K, Sakakura C, Li QL *et al.* RUNX3 suppresses gastric epithelial cell growth by inducing p21(WAF1/Cip1) expression in cooperation with transforming growth factor {beta}-activated SMAD. *Mol Cell Biol* 2005; **25**: 8097–8107.
30 Li QL, Ito K, Sakakura C, Fukamachi H, Inoue K, Chi XZ *et al.* Causal relationship between the loss of RUNX3 expression and gastric cancer. *Cell* 2002; **109**: 113–124.
31 Gustafson WC, Weiss WA. Myc proteins as therapeutic targets. *Oncogene* 2010; **29**: 1249–1259.
32 Otto T, Horn S, Brockmann M, Eilers U, Schuttrumpf L, Popov N *et al.* Stabilization of N-Myc is a critical function of Aurora A in human neuroblastoma. *Cancer Cell* 2009; **15**: 67–78.
33 Salghetti SE, Kim SY, Tansey WP. Destruction of Myc by ubiquitin-mediated proteolysis: cancer-associated and transforming mutations stabilize Myc. *EMBO J* 1999; **18**: 717–726.
34 Fredlund E, Ringner M, Maris JM, Pahlman S. High Myc pathway activity and low stage of neuronal differentiation associate with poor outcome in neuroblastoma. *Proc Natl Acad Sci USA* 2008; **105**: 14094–14099.
35 Chen L, Iraci N, Gherardi S, Gamble LD, Wood KM, Perini G *et al.* p53 is a direct transcriptional target of MYCN in neuroblastoma. *Cancer Res* 2008; **70**: 1377–1388.
36 Lasorella A, Noseda M, Beyna M, Yokota Y, Iavarone A. Id2 is a retinoblastoma protein target and mediates signalling by Myc oncoproteins. *Nature* 2000; **407**: 592–598.
37 Slack A, Chen Z, Tonelli R, Pule M, Hunt L, Pession A *et al.* The p53 regulatory gene MDM2 is a direct transcriptional target of MYCN in neuroblastoma. *Proc Natl Acad Sci USA* 2005; **102**: 731–736.
38 Guo WH, Weng LQ, Ito K, Chen LF, Nakanishi H, Tatematsu M *et al.* Inhibition of growth of mouse gastric cancer cells by Runx3, a novel tumor suppressor. *Oncogene* 2002; **21**: 8351–8355.
39 Yano T, Ito K, Fukamachi H, Chi XZ, Wee HJ, Inoue K *et al.* The RUNX3 tumor suppressor upregulates Bim in gastric epithelial cells undergoing transforming growth factor beta-induced apoptosis. *Mol Cell Biol* 2006; **26**: 4474–4488.
40 Sjostrom SK, Finn G, Hahn WC, Rowitch DH, Kenney AM. The Cdk1 complex plays a prime role in regulating N-myc phosphorylation and turnover in neural precursors. *Dev Cell* 2005; **9**: 327–338.
41 Tomioka N, Oba S, Ohira M, Misra A, Fridlyand J, Ishii S *et al.* Novel risk stratification of patients with neuroblastoma by genomic signature, which is independent of molecular signature. *Oncogene* 2008; **27**: 441–449.
42 Takenobu H, Shimozato O, Nakamura T, Ochiai H, Yamaguchi Y, Ohira M *et al.* CD133 suppresses neuroblastoma cell differentiation via signal pathway modification. *Oncogene* **30**: 97–105.

Supplementary Information accompanies this paper on the Oncogene website (http://www.nature.com/onc)

VOLUME 32 · NUMBER 12 · APRIL 20 2014

JOURNAL OF CLINICAL ONCOLOGY

ORIGINAL REPORT

Metastatic Neuroblastoma Confined to Distant Lymph Nodes (stage 4N) Predicts Outcome in Patients With Stage 4 Disease: A Study From the International Neuroblastoma Risk Group Database

Daniel A. Morgenstern, Wendy B. London, Derek Stephens, Samuel L. Volchenboum, Barbara Hero, Andrea Di Cataldo, Akira Nakagawara, Hiroyuki Shimada, Peter F. Ambros, Katherine K. Matthay, Susan L. Cohn, Andrew D.J. Pearson, and Meredith S. Irwin

Daniel A. Morgenstern and Meredith S. Irwin, Hospital for Sick Children and University of Toronto; Derek Stephens, Hospital for Sick Children, Toronto, ON, Canada; Daniel A. Morgenstern, Great Ormond Street Hospital for Children National Health Service (NHS) Foundation Trust, London; Andrew D.J. Pearson, The Royal Marsden NHS Foundation Trust, Sutton, Surrey, United Kingdom; Wendy B. London, Dana-Farber/Boston Children's Cancer and Blood Disorders Center, Boston, MA; Samuel L. Volchenboum and Susan L. Cohn, University of Chicago, Chicago, IL; Barbara Hero, University Children's Hospital, Köln, Germany; Andrea Di Cataldo, University of Catania, Catania, Italy; Akira Nakagawara, Chiba University School of Medicine, Chiba, Japan; Hiroyuki Shimada, University of Southern California at Los Angeles, Los Angeles; Katherine K. Matthay, University of California at San Francisco, San Francisco, CA; and Peter F. Ambros, St. Anna Kinderkrebsforschung, Vienna, Austria.

Published online ahead of print at www.jco.org on March 24, 2014.

Terms in blue are defined in the glossary, found at the end of this article and online at www.jco.org.

Presented at the 49th Annual Meeting of the American Society of Clinical Oncology, Chicago, IL, May 31-June 4, 2013.

Authors' disclosures of potential conflicts of interest and author contributions are found at the end of this article.

Corresponding author: Meredith Irwin, MD, Division of Haematology/Oncology, The Hospital for Sick Children, 555 University Avenue, Toronto, ON, Canada M5G 1X8; e-mail: meredith.irwin@sickkids.ca.

0732-183X/14/3212w-1228w/$20.00

DOI: 10.1200/JCO.2013.53.6342

ABSTRACT

Purpose
The presence of distant metastases is one of the most powerful predictors of outcome in patients with neuroblastoma. However, the pattern of metastatic spread is not incorporated into current risk stratification systems. Small case series have suggested that patients with neuroblastoma who have metastatic disease limited to distant lymph nodes (4N disease) may have improved outcomes.

Patients and Methods
We analyzed retrospective data from the International Neuroblastoma Risk Group database for patients diagnosed from 1990 to 2002. 4N patients were compared with the remaining stage 4 patients (non-4N), excluding those with missing metastatic site data.

Results
In all, 2,250 International Neuroblastoma Staging System stage 4 patients with complete data were identified, of whom 146 (6.5%) had 4N disease. For 4N patients, event-free survival (EFS; 5-year, 77% ± 4%) and overall survival (OS; 5-year, 85% ± 3%) were significantly better than EFS (5-year, 35% ± 1%) and OS (5-year, 42% ± 1%) for non-4N stage 4 patients ($P < .001$). 4N patients were more likely to be younger ($P < .001$) and have tumors with favorable characteristics, including absence of *MYCN* amplification (89% *v* 69%; $P < .001$). In a multivariable analysis, 4N disease remained a significant predictor of outcome (hazard ratio for non-4N *v* 4N: 3.40 for EFS and 3.69 for OS). Within subgroups defined by age at diagnosis and tumor *MYCN* status, 4N disease was significantly associated with improved outcomes.

Conclusion
4N represents a subgroup with better outcome than that of other patients with metastatic disease. These findings suggest that the biology and treatment response of 4N tumors differ from other stage 4 tumors, and less intensive therapy should be considered for this cohort. Future exploration of biologic factors determining the pattern of metastatic spread is warranted.

J Clin Oncol 32:1228-1235. © 2014 by American Society of Clinical Oncology

INTRODUCTION

Risk stratification is a key principle of current neuroblastoma treatment protocols, and therapy is determined by prognostic factors, including patient age, tumor stage, histology, ploidy, and *MYCN* amplification (MNA) status.[1] The value of incorporating additional genetic markers (ie, segmental chromosome aberrations [SCAs] such as loss of 11q) is currently being explored. Patients older than age 18 months with metastatic (stage 4) disease, most commonly involving bone and bone marrow, typically have a poor prognosis despite intensive multimodal therapy.[1] Although the prognostic significance of metastatic spread to specific sites has not been extensively studied, case reports and small case series have raised the possibility that patients with metastatic disease confined to distant lymph nodes (4N disease; previously IV-N) may have a better outcome.[2-6]

In a single-institution series of six patients with Evans stage IV neuroblastoma and extensive lymph node metastases but no extranodal disease, three patients were long-term survivors in comparison to none of the 40 patients with standard stage IV disease (extranodal involvement).[2] Subsequently,

Yamada et al[3] reported 52 patients with stage III to IV disease, of whom eight had N3 disease (distant nodal involvement). Three of these had metastatic disease that was limited to nodal sites. Among patients with stage IV disease, there was a trend toward better overall survival (OS) in those with N3 disease compared with other groups. There was also a trend toward an association between N3 stage IV disease and the absence of MNA (zero of four MNAs) compared with other stage IV patients (11 of 22 MNAs). Abramson et al[4] reported a series of eight patients with abdominal primary tumors and specific distant node involvement of the left supraclavicular lymph nodes (Virchow's node). Four were long-term survivors (3 to 11 years). In a separate case report, a 10-year-old patient with stage IV-N, non-MNA neuroblastoma was also a long-term survivor.[5] In an analysis of the prognostic impact of different metastatic sites in 434 patients older than 1 year of age with stage 4 neuroblastoma, 11 patients (2.5%) had 4N disease, with a nonsignificant trend toward improved event-free survival (EFS) for these individuals.[6] Loss of heterozygosity (LOH) at 19q13 has been suggested as a marker for locoregional disease with reported increased frequency in patients with stage 3 or stage 4N disease.[7] In that series, 19q LOH was detected in four (67%) of six stage 4N patients but in only four (7%) of 55 non-4N stage 4 patients. Finally, in an analysis of 218 patients with stage 4 disease treated with high-dose chemotherapy and stem-cell rescue, Hartmann et al[8] reported the absence of bone marrow metastases at diagnosis as a favorable prognostic marker, although it is important to note that these patients cannot be formally identified as stage 4N (ie, they may have had extralymphatic metastases to other sites).

The International Neuroblastoma Risk Group (INRG) database brings together patient data from groups in North America, Europe, Australia, and Japan and is the largest single source of data on neuroblastoma, containing information on more than 8,800 children.[1] This resource therefore provides a unique opportunity to establish whether stage 4N neuroblastoma represents a defined subgroup of patients with metastatic disease and to examine differences in prognostic factors and outcome for this rare cohort.

PATIENTS AND METHODS

Patient Cohort

The INRG database includes data from the Children's Oncology Group (COG; North America/Australia), Society of Paediatric Oncology European Neuroblastoma Group (SIOPEN; predominantly Europe), German, and Japanese cooperative study groups. Patients age younger than 21 years with pathologically confirmed neuroblastoma diagnosed between January 1, 1990, and December 31, 2002, are currently included. Of the total 8,800 patients, 3,244 (37%) had stage 4 disease. Of these, 994 were excluded because of incomplete or inconsistent metastatic site data, leaving 2,250 patients in the final analytic cohort (26% of all patients in the database). Patient age, site of primary tumor, and follow-up data were available for all patients. Other variables, including serum ferritin, lactate dehydrogenase (LDH), MNA, and cytogenetic characteristics, were analyzed for those patients for whom data were available. Histology was classified as favorable or unfavorable according to International Neuroblastoma Pathology Classification (INPC) or the Shimada system.[1,9] The cohort of 4N patients was defined as those with positive distant lymph nodes, but no bone marrow, bone, liver, lung, CNS, skin, or other metastatic disease. Patients with missing or unknown pattern of metastatic disease were excluded. The INRG uses International Neuroblastoma Staging System (INSS)[10] or Evans stage[11] if INSS unknown, as the staging criteria.[1,12] Consequently, patients with regional lymph node involvement were not considered to have metastatic disease and thus do not meet criteria for inclusion in this analysis.

Statistical Methods

Time to event for EFS was defined as time from diagnosis to first relapse, progression, second malignancy, or death or until time of last contact if no event occurred. Time to event for OS was similarly defined as time from diagnosis to death or time of last contact if patient was alive. Estimates for 5-year EFS and OS were generated by using the Kaplan-Meier method, and curves were compared by using a log-rank test.[13] For univariable analyses to identify factors prognostic of EFS or OS, a 5% significance level was used without adjustment for multiple testing, except for primary tumor site for which Sidak adjustment for multiple comparisons was used. Patient characteristics and prognostic factors were compared by using t test or Mann-Whitney U test for continuous variables and Fisher's exact test or χ^2 test for binary or other categorical variables as appropriate. Variables such as age, LDH, and ferritin were dichotomized as per previous INRG database analyses.[1,14] Cox proportional hazards regression models were used to identify the most significant factors prognostic of outcome in multivariable analyses.

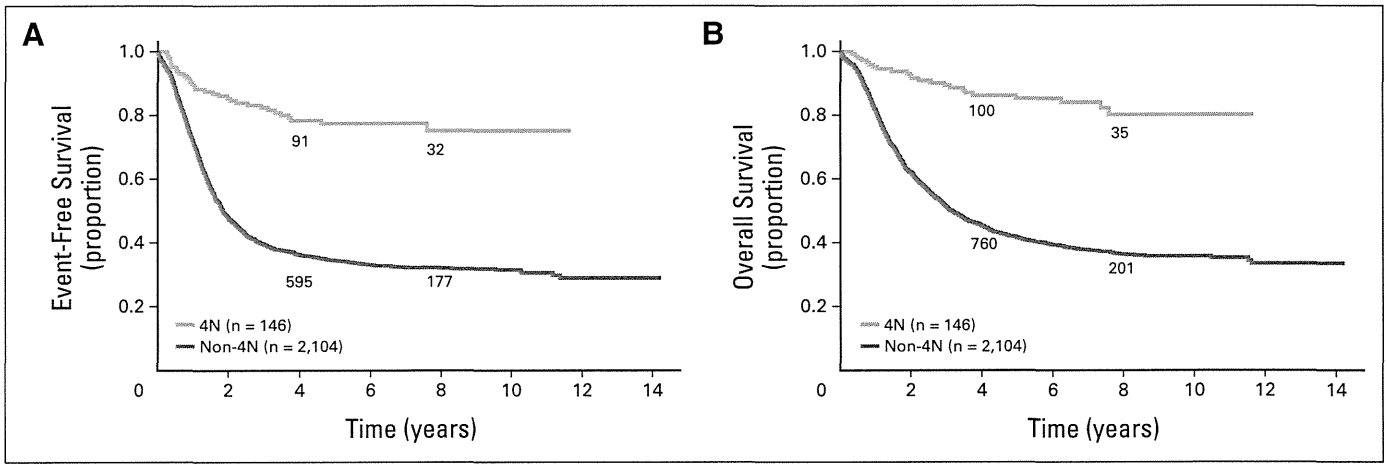

Fig 1. Patients with stage 4 neuroblastoma. (A) Event-free survival and (B) overall survival curves for patients with 4N disease (metastatic spread limited to distant lymph nodes) versus the balance of stage 4 patients (non-4N). $P < .001$ for both event-free and overall survival. The numbers of patients at risk for an event are shown along the curves at years 4 and 8.

RESULTS

Stage 4N Cohort

Data from 3,244 patients with stage 4 disease from the INRG database were analyzed. Those with missing or inconsistent data relating to metastatic site (n = 994) were excluded, leaving a final cohort of 2,250 patients. Comparison of EFS and OS showed that these excluded patients had a significantly worse outcome compared with the final analytic cohort ($P = .0024$ for EFS; $P < .001$ for OS; Figure A1, online only). Of the final group, 146 (6.5%) had a 4N pattern of disease (metastatic spread limited to distant lymph nodes), and the remaining 2,104 non-4N stage 4 patients served as the comparison cohort. For the 4N patients, estimated 5-year EFS and OS were 77% ± 4% and 85% ± 3%, both significantly better than those for non-4N stage 4 patients (EFS, 35% ± 1%; OS, 42% ± 1%; $P < .001$ for both EFS and OS; Fig 1). Comparison of clinical features demonstrated important differences between the two groups (Table 1; Appendix Table A1, online only). Stage 4N patients were younger (median age, 423 *v* 929 days; $P < .001$) and had tumors with more favorable histology, including INPC/Shimada histologic classification, grade of tumor differentiation, and mitosis karyorrhexis index (MKI). MNA was less frequent in stage 4N patients (11% *v* 31%; $P < .001$). Other cytogenetic features, including ploidy, 1p or 11q loss, or 17q gain, were not significantly different between the 4N and non-4N groups, although data were unavailable for many patients (see Appendix, online only). Patients with 4N disease were less likely to have an adrenal primary (40% *v* 60% $P < .001$) and more likely to have a thoracic tumor (26% *v* 10%; $P < .001$), consistent with increased frequency of thoracic primary tumors in patients age younger than 547 days.[15] Within the total stage 4 population, primary tumor was thoracic in 15% of patients age younger than 547 days versus 9.9% in those age ≥ 547 days ($P < .001$). Consistent with the more favorable outcome observed, 4N patients also had lower mean serum ferritin (147 *v* 324 ng/mL; $P < .001$) and LDH (1,207 *v* 1,763 U/L; $P = .0192$). Year of diagnosis was earlier for patients with 4N disease, with 77% diagnosed before 1996 (*v* 63% for non-4N patients; $P < .001$). In terms of therapy, 4N patients were less likely to receive intensive initial therapy than non-4N patients; therefore treatment differences are unlikely to account for the improved outcome of the 4N group (Appendix Table A2, online only).

The importance of the 4N pattern of disease as a prognostic factor was explored in a multivariable analysis by using Cox proportional hazards. A model incorporating known prognostic variables (INSS stage, age, *MYCN* status, year of diagnosis, serum ferritin, and LDH) for which adequate data were available (n = 952) confirmed that stage 4N is independently statistically significantly prognostic of improved EFS and OS after adjusting for these variables (Table 2). Similar results were obtained after the incorporation of histology, ploidy, grade, MKI, and 11q, 1p, and 17q status into the model, each with a category for unknown (Appendix Table A3, online only). The Cox model was also used to calculate the hazard ratios for stage 4N versus non-4N (range, 0.24 to 0.36) when tested individually with each prognostic factor in separate models (Appendix Table A4, online only).

Table 1. Comparison of Characteristics for 4N and Non-4N Stage 4 Patients

Characteristic	4N (n = 146) No.	4N (n = 146) %	Non-4N (n = 2,104) No.	Non-4N (n = 2,104) %	*P*
Age					
Median, days	423		929		< .001
< 18 months	85	58	640	30	
≥ 18 months	61	42	1,464	70	< .001
Year of diagnosis					
1990-1995	113	77	1,314	62	
1996-2002	33	23	790	38	< .001
Ferritin/LDH (± SD)					
Mean ferritin, ng/mL	147 ± 261		324 ± 461		< .001
Mean LDH, U/L	1,207 ± 1,859		1,763 ± 2,236		.0192
Histologic category					
Favorable	45	63	219	26	
Unfavorable	27	37	609	74	< .001
Histologic grade					
Differentiating	9	21	44	8	
Undifferentiated/poorly differentiated	33	79	537	92	.0058
MKI					
Low	28	76	240	45	
Intermediate	6	16	158	29	
High	3	8	138	26	.0011
MYCN status					
Nonamplified	120	89	1,145	69	
Amplified	15	11	511	31	< .001
Cytogenetics					
Ploidy					
Hypodiploid/diploid	22	27	231	38	
Hyperdiploid	60	73	385	62	.0666
1p loss					
Yes	7	35	183	36	
No	13	65	318	64	1.0
17q gain					
Yes	3	50	100	64	
No	3	50	57	36	.6703
11q loss					
Yes	3	30	114	42	
No	7	70	154	58	.5270
Site of primary*					†
Adrenal	59	40	1273	60	< .001
Abdomen	38	26	498	24	N/S
Neck	6	4	25	1	N/S
Thorax	38	26	220	10	< .001
Pelvis	3	2	28	1	N/S
Other	4	2	78	4	N/S
Initial treatment					
None/surgery/conventional	71	77	502	30	
Intensive ± SCT	21	23	1168	70	< .001

Abbreviations: LDH, lactate dehydrogenase; MKI, mitosis karyorrhexis index; N/S, not significant; SCT, stem cell transplantation; SD, standard deviation.
*A small number of patients had primary tumors in multiple sites; therefore, totals vary from actual number of individual patients.
†*P* values corrected by using Sidak adjustment for multiple comparisons.

Prognostic Factors Within 4N Cohort

Many of the factors previously reported to affect outcome within the whole neuroblastoma population were also prognostic when examined within the 4N cohort (Table 3). Most significant in a univariable analysis for factors determining OS were patient age (using a cutoff at 547 days[14]; $P < .001$), tumor MNA status ($P < .001$), and INPC/Shimada histology classification ($P < .001$). Serum ferritin, LDH, tumor MKI, and initial treatment were also significant at the 5%

Table 2. Multivariable Cox Proportional Hazards Models (one model for EFS and one for OS) in 952 Patients Who Had Complete Data

	EFS			OS		
Risk Factor*	HR	95% CI	*P*	HR	95% CI	*P*
Stage						
4N disease	1	—		1	—	
Non-4N disease	3.40	2.00 to 5.81	< .001	3.69	2.02 to 6.71	< .001
Year of diagnosis						
1996-2002	1	—		1	—	
1990-1995	1.29	1.09 to 1.51	< .001	1.34	1.13 to 1.59	< .001
Age at diagnosis, days						
< 547	1	—		1	—	
≥ 547	2.16	1.74 to 2.68	< .001	2.25	1.79 to 2.84	< .001
MYCN amplification						
Nonamplified	1	—		1	—	
Amplified	1.76	1.47 to 2.10	< .001	1.93	1.60 to 2.32	< .001
Serum ferritin, ng/mL						
< 92	1	—		1	—	
≥ 92	1.54	1.26 to 1.89	< .001	1.48	1.19 to 1.84	< .001
Serum LDH, U/L						
< 580	1	—		1	—	
≥ 580	1.32	1.08 to 1.60	.0062	1.58	1.27 to 1.95	< .001

Abbreviations: EFS, event-free survival; HR, hazard ratio; LDH, lactate dehydrogenase; OS, overall survival.
*Other risk factors (histology, grade, mitosis karyorrhexis index, and ploidy) were not included in the model because missing data dramatically reduced the sample size and the model became uninformative.

level. Year of diagnosis was not correlated with outcome within the 4N cohort.

Subgroup Analysis

Because age and presence of MNA are independently prognostic of outcome within the INSS stage 4 population and are used for risk stratification within current international studies, we further evaluated the prognostic significance of 4N disease pattern in four subgroups defined by patient age (cutoff, 547 days) and tumor *MYCN* status. 4N patients had significantly improved EFS and OS compared with non-4N patients in each subgroup (Fig 2), except for patients age younger than 547 days with MNA tumors, a subgroup in which there were only four stage 4N patients. For patients age younger than 547 days with non-MNA tumors, 5-year EFS and OS were 92% ± 3% and 99% ± 1% for 4N disease compared with 83% ± 2% and 88% ± 2% for non-4N disease ($P = .03$ and $P = .004$, respectively; Fig 2A). The differences were more pronounced for patients age ≥ 547 days with non-MNA tumors; estimated 5-year EFS and OS were 63% ± 8% and 74% ± 7% for those with 4N disease, both significantly better than for non-4N patients (EFS, 27% ± 2%; OS, 38% ± 2%; $P < .001$ for both EFS and OS; Fig 2B). Within this subgroup of patients age ≥ 547 days with non-MNA tumors, comparison of characteristics between 4N and non-4N patients revealed no differences in patient age or site of primary tumor. However, patients with 4N disease were more likely to have tumors with favorable histologic characteristics, including Shimada/INPC classification, grade, and MKI (Table 4). Insufficient data were available to allow comparison of tumor ploidy or incidence of SCAs between 4N and non-4N patients. Finally, in the subgroup of patients age ≥ 547 days with MNA tumors, 5-year EFS and OS were again better for 4N patients (both 64% ± 15%) than for non-4N patients (EFS, 17% ± 2% [$P = .0133$]; OS, 22% ± 2% [$P = .0278$]).

DISCUSSION

Numerous prognostic factors for neuroblastoma have been identified, including patient characteristics (particularly age at diagnosis), disease extent (INSS stage), and tumor biology. The most significant predictive genetic factors are MNA[1,16] and SCAs, including 1p and 11q deletions.[17,18] For patients with stage 4 disease, the pattern of metastatic spread may also influence outcome, and several case reports and small case series have suggested that patients with only distant nodal metastatic involvement (4N disease) may have better outcomes.[2-5] Although an analysis of the prognostic significance of specific metastatic sites demonstrated that the presence of bone marrow metastases was predictive of poor outcome,[19] this report did not examine outcomes for patients with disease limited to a particular metastatic site, such as lymph nodes.

The INRG database represents the largest data set for patients with neuroblastoma, and the analysis presented here provides the most comprehensive analysis of 4N patients to date. These data demonstrate that patients with 4N disease have a markedly better outcome compared with other stage 4 patients. Although published cases suggested that 4N disease may be more common in older patients (median age of published cases, 4 years), this is not supported by our larger data set, in which more than half of 4N patients were infants age younger than 18 months. 4N disease is inversely correlated with MNA and, consequently, the prognostic significance of 4N disease can be at least partly explained by the association with younger age and absence of MNA—both factors strongly associated with improved outcome in stage 4 disease.[1] Nevertheless, both the subgroup and multivariable analyses confirm that 4N disease remains independently associated with improved outcome even after adjusting for age and *MYCN* status. The hazard ratio for non-4N disease (compared with 4N) of

Table 3. Univariable Analyses of Prognostic Factors for 4N Patients

Characteristic	Total		5-Year EFS			5-Year OS		
	No.	%	%	SE	*P*	%	SE	*P*
Overall patients	146		77	4		85	3	
Age, days								
< 547	85	58	91	3	< .001	98	2	< .001
≥ 547	61	42	59	6		69	6	
Year of diagnosis								
1990-1995	113	77	78	4	.7646	86	3	.5466
1996-2002	33	23	77	8		82	8	
MYCN status								
Nonamplified	120	89	81	4	.0172	90	13	< .001
Amplified	15	11	64	13		63	3	
Ferritin, ng/mL								
< 92	38	49	89	6	.0012	93	5	.0021
≥ 92	39	51	62	8		70	8	
LDH, U/L								
< 580	43	46	79	7	.1842	92	4	.0273
≥ 580	50	54	73	7		74	7	
Ploidy								
Hyperdiploid	60	73	82	5	.2485	89	4	.0776
Diploid/hypodiploid	22	27	73	10		73	11	
Histology								
Favorable	45	62	89	5	.0127	98	2	< .001
Unfavorable	27	38	61	10		68	10	
Histologic grade								
Differentiating	9	21	78	14	.9454	100		.0864
Undifferentiated/poorly differentiated	33	79	74	8		76	8	
MKI								
Low/intermediate MKI	34	92	79	7	.0407	87	6	.0062
High MKI	3	8	33	27		33	27	
Initial treatment								
None/surgery only	35	38	91	5		97	3	
Conventional chemotherapy	36	39	80	7		91	5	
Intensive ± SCT	21	23	59	11	.0065	69	10	.0024

Abbreviations: EFS, event-free survival; LDH, lactate dehydrogenase; MKI, mitosis karyorrhexis index; OS, overall survival; SCT, stem cell transplantation; SE, standard error.

approximately 3.5 for both EFS and OS is larger than for any of the other variables tested, which demonstrates that this metastatic pattern is powerfully prognostic of outcome within the stage 4 population. The overall frequency of 4N disease is low (6.5% of stage 4 patients); however, the risk reduction associated with 4N disease suggests that this metastatic pattern may need to be considered differently within the current risk stratification system. Recent efforts have attempted to identify subgroups of high-risk patients with the poorest outcomes, so-called "ultra-high-risk patients." Our findings suggest that, in contrast, there may also be subsets of patients such as those with 4N disease in which further treatment intensification may not be warranted or treatment reduction may be considered. Current standard therapy for high-risk patients includes chemotherapy, surgery, myeloablative therapy with stem-cell rescue, radiotherapy, immunotherapy, and differentiation therapy and is associated with significant short- and long-term toxicities. The definition of high-risk disease has already undergone several revisions, with it long being recognized that infants (age younger than 12 months) with neuroblastoma have a considerably better outcome, even if presenting with metastatic disease.[11] Consequently, these patients (provided their disease does not have MNA) are not considered high risk. More recently, the definition of high-risk disease has been further refined with those age 12 to 18 months with non-MNA metastatic disease (approximately 6% of all stage 4 patients) also excluded from the high-risk group.[1,14] Patients older than age 18 months with 4N disease may represent another subgroup that could be reclassified.

The improved outcome for 4N patients likely represents underlying biologic differences in the tumor, with pattern of metastatic spread being a surrogate marker for these differences. Comparison of histologic features between 4N and non-4N populations (within both the entire cohort and in subgroups of patients age ≥ 547 days and without MNA) confirmed that 4N disease is associated with differentiating grade, low MKI, and favorable histology, all characteristics of a more favorable tumor biology.[20] Ultimately, these variables likely reflect underlying genetic and chromosomal abnormalities, and 4N tumors may have a specific pattern of these abnormalities that distinguish them from other stage 4 neuroblastoma. There is limited cytogenetic information within the current INRG data set, and numbers were insufficient to demonstrate associations among 1p and 11q loss, 17q gain, or other SCAs and the 4N pattern of disease (see Appendix). Many preclinical studies and gene expression analyses in cancers, including breast cancer and melanoma, have demonstrated that specific messenger RNA expression signatures predict patterns or sites of

